The pathophysiological effects of Russell's viper (*Daboia siamensis*) venom and its fractions in the isolated perfused rabbit kidney model: A potential role for platelet activating factor

Narongsak Chaiyabutr [a,*], Lawan Chanhome [a], Taksa Vasaruchapong [a], Panithi Laoungbua [a], Orawan Khow [a], Anudep Rungsipipat [b], Visith Sitprija [a]

[a] *Queen Saovabha Memorial Institute, The Thai Red Cross Society, Bangkok, 10330, Thailand*
[b] *Department of Veterinary Pathology, Faculty of Veterinary Science, Chulalongkorn University, Bangkok, 10330, Thailand*

ARTICLE INFO

ABSTRACT

The pathophysiological effects of Russell's viper venom (RVV) and its fractions, including phospholipase A_2 (RvPLA$_2$), metalloprotease (RvMP), L-amino acid oxidase (RvLAAO), and phosphodiesterase (RvPDE) on renal functions were investigated using the isolated perfused rabbit kidney (IPK) model. Moreover, whether their effects on renal alterations were promoted by platelet activating factor (PAF) was tested using the PAF receptor antagonist, WEB 2086. There was a marked reduction in the perfusion pressure (PP) and renal vascular resistance (RVR) 10 min after RVV administration (1.0 mg/100 ml of perfusate), thereafter both PP and RVR gradually increased and approached the control level within 90 min. These effects were abolished by pretreatment with WEB2086 (2 µg/µl). Administration with RvPLA$_2$ (280 µg/ml), RvMP (280 µg/ml), or RvLAAO (135 µg/ml) alone increased both the PP and RVR, whereas RvPDE (100 µg/ml) reduced both the PP and RVR. Pretreatment with WEB 2086 completely abolished the effects induced by RvMP, but not the other fractions. The RVV also caused a marked decrease in the glomerular filtration rate (GFR), urinary flow rate (UF), and osmolar clearance (Cosm), and these effects were not inhibited by pretreatment with WEB2086. Each RVV fraction also increased, to varying extents, the GFR, UF, and Cosm, and these effects induced by RvPLA$_2$ or RvMP, but not the other fractions, were completely blocked by WEB 2086. Changes in percent filtered Na^+ and K^+ excreted in the IPK by RVV, RvPDE, and RvMP were abolished by pretreatment with WEB 2086. Histological evaluation profiled mainly tubulonephrosis in the treated kidney. These results reveal that the alterations in renal functions induced by RVV and its fractions are due to the synergistic action of the different components of snake venom, instead of the action of a single component. The effects of RVV and its fractions in rabbit IPK are mediated at least in part by PAF.

1. Introduction

Snakebite is an important public health problem in several countries in the tropics, and amongst these Russell's viper (*Daboia siamensis*) causes a high morbidity and mortality. The main and most serious complication following Russell's viper bite is acute kidney injury (AKI) (Kanjanabuch and Sitprija, 2008). The mechanisms acting within the body to induce AKI during envenomation are uncertain. The pathogenetic mechanisms underlying acute renal failure (ARF) may include renal vascular obstruction by disseminated intravascular coagulation (DIC), ischemia or hypoperfusion due to the fall in blood pressure, and

some extent of intravascular hemolysis lead to pigment nephropathy (Sitprija et al., 1974). This manifestation does not exclude the presence of proteolytic enzymes and vasoactive substances, which could promote, or even potentiate, the coagulant process in renal sites. *In vivo* studies in experimental animals have shown that decreases in the renal blood flow (RBF) and the glomerular filtration rate (GFR) with an injection of the crude venom of Russell's viper (RVV) might be depend on changes in extrarenal factors via reductions in both the systemic and renal circulations (Tungthanathanich et al., 1986; Thamaree et al., 1994).

The etiology of RVV induced ARF in humans and experimental animals is still not completely understood but probably involves the direct

---

action of the venom components on the renal tubules and renal epithelial cells (Sitprija and Chaiyabutr, 1999). The possible existence of a direct nephrotoxic component was reported, but has not been well described up to now. Overall, RVV is a complex mixture that contains both non-protein and protein components with different structures and specific biochemical activities. The major protein components of RVV consist of a mixture of potentially toxic proteins, peptides, and several enzymes (Tan et al., 2018). The possible effect of each venom component may dominate the clinical presentation causing local and systemic injury as well as haematological, cardiovascular, and renal functions.

The isolation and functional characterization of venom components will provide a basis for understanding the mechanisms and/or molecular models of venom action (Harvey et al., 1998). However, the potential role of each venom component of RVV, direct and/or indirect, in the cytotoxicity related to AKI has not been studied in as much detail. Previous studies done in experimental animals by Suwansrinon et al. (2007) demonstrated that administration of the phospholipase A2 (PLA$_2$) or metalloprotease (MP) fractions of RVV caused alterations in the renal functions, where changes in the renal hemodynamics appeared to correlate better with the MP than PLA$_2$ component of the RVV. In addition, Mitrmoonpitak et al. (2013) reported that injection of the venom fraction (either PLA$_2$ or MP) promoted intense inflammatory mediators with an elevation of plasma concentrations of pro-inflammatory cytokines for interleukin-6, tumor necrosis factor-α, and prostaglandin E2 (PGE2). The plasma level of nitric oxide (NO), a vasoactive mediator, was increased after injection with the PLA$_2$ fraction but not with the MP fraction. The question is which venom fraction promotes more inflammatory mediators and which venom fraction plays a key role in its effects for such responses. These *in vivo* models do not exclude the influence of a higher order of extrarenal factors, such as the nervous system, blood pressure, coagulation, and other blood borne factors, including corpuscles and hormones. However, few data are available to study the specific mechanisms in responsible for the induction of AKI by RVV and its fractions, although a number of studies have reported the direct effects of RVV on renal tubular and glomerular injury in the isolated perfused kidney (IPK) model (Ratcliffe et al., 1989; Willinger et al., 1995; Chaiyabutr et al., 2014).

Nevertheless, ARF can result from a variety of renal injuries and several processes that make a major contribution to the reduction in the GFR and RBF, which are characteristic of ARF. It has been reported that the kidney is capable of releasing inflammatory mediators in response to several stimuli (Pirotzky et al., 1984b), but the search for a factor(s) locally released into the kidney during envenomation that might be responsible for the changes in the renal vascular and glomerular functions associated with renal failure is still an ongoing research area. The release of intrarenal factors in envenoming may be superimposed on the renal effects of the investigated venom action. It has been demonstrated that platelet activating factor (PAF), an acetylated alkyl phosphoglycerides and lipid mediator, can be released by several cell types such as eosinophil (Benveniste et al., 1972) and organ, including the kidney (Caramelo et al., 1984). Of interest, PAF is a membrane-derived phospholipid with widely recognized pro-inflammatory activities and may be one of the entities responsible for causing the hemodynamic changes in ARF, because it can act as a vasodilator or vasoconstrictor, depending upon its concentration (Lo'pez-Novoa, 1999).

The implication of PAF as an important pro-inflammatory mediator in the pathogenesis of ARF involves on PAF levels in the kidney, which has been supported by the study of Caramelo et al. (1984), who reported the presence of PAF in blood from normal human and experimental animals, but not in blood from anephric patients or bilaterally nephrectomized animals. It has been reported that PAF also plays an essential role in signal transduction pathways for induction of NO production, which acts as a mediator exerting a vasodilator activity on afferent arterioles (Juncos et al., 1993). However, there are no studies evaluating the role of PAF during envenomation with RVV, although PAF is an important mediator in the reduction of GFR and urinary flow rate (UF)

induced by the venom of *Bothrops* snakes, which are blocked by the specific PAF receptor antagonist WEB 2086 in the rat IPK model (Monteiro and Fonteles, 1999; Havt et al., 2001).

Considering the above data, whether the pathogenesis of ARF induced by RVV involves the local generation of PAF in the kidney is not fully understood. We, therefore, hypothesized that the action of venom, either RVV or its venom fractions, to cause renal functional alterations would involve the PAF pathway in the kidney. We decided to study whether the nephrotoxic effect of RVV and its fractions is somehow related to a concomitant generation of PAF and the specific PAF receptor antagonists WEB 2086, a powerful *in vitro* antagonists of PAF receptor (Casals-Stenzel and Heuer, 1990), is essential to evaluate for such studies.

Because RVV consists of a mixture of several toxic enzymes, the nephrotoxic effect of RVV cannot formally exclude a potential interference of AKI with the function of other venom components. Thus, in the present study, additional comparative studies of renal alterations caused by RVV and its fractions were performed in order to confirm the precise role of each venom fraction in the IPK. Generation of PAF in the kidney might involve the action of RVV via any of its components. Moreover, since the study of the mechanisms of action of venom fractions for the pathogenesis of ARF is difficult *in vivo*, the *in vitro* studies in the IPK model without the influence of extrarenal factors would help in this regard.

Therefore, two experimental protocols were performed. The first protocol was performed to characterize the functional properties of PAF in the rabbit IPK using two different concentrations of exogenous PAF and confirmation of its function with pre-exposure to WEB 2086 as a blocker. The second protocol was designed as a comparative study on the direct renal effects promoted by RVV and its isolated PLA$_2$ (RvPLA$_2$), MP (RvMP), L-amono acid oxidase (RvLAAO), and phoshodiesterse (RvPDE) fractions. The role of local PAF generation during envenoming was tested by pretreatment with WEB 2086 in the rabbit IPK model. After treatment with RVV or a respective venom fraction, with or without a 30-min pretreatment with WEB 2086, the renal histological examinations were verified. Defining the role of PAF in modulating the action of RVV and its venom fractions in the rabbit IPK model without the influence of extrarenal factors will lead to a better understanding of these pathophysiological mechanisms involved in the features of AKI.

2. Materials and methods

2.1. Experimental animals

Adult male white New Zealand rabbits, weighing 2–3 kg, were obtained from the Animal house, Queen Saovabha Memorial Institute. The animals were settled in stainless steel cages, fed a standard diet and water, exposed to a 12 h light/dark cycle, and maintained at a laboratory temperature of 26 ± 1 °C. The animals were quarantined for 14 d before experiments. Animal experiments involved in this study were conducted with permission of the Ethics Committee of the Queen Saovabha Memorial Institute Animal Care and Use (approval number QSMI-ACUC-03-2016) in accordance with the guideline of the National Research Council of Thailand.

2.2. Preparation of the rabbit IPKs

Preparation of the rabbit IPK was based on the previously described method (Chaiyabutr et al., 2014). Briefly, adult male white New Zealand rabbits were fasted 24 h before the experiment with access to water ad libitum. The rabbit was anaesthetized with pentobarbital sodium (30 mg/kg body weight, iv). The left kidney was prepared for perfusion after careful dissection. The animal was given 1000 units heparin intravenously and the left ureter was cannulated with a polyvinyl catheter. The kidney was cannulated through the renal artery directly with a 19-gauge stainless steel needle, approximately 1.0 inch in length with a smooth

tip, and immediately flushed with heparinized saline (100 units/ml). The kidney was isolated with the renal vein and the ureter intact and then immediately transferred to a thermostatically controlled tissue bath organ chamber (Radnoti, chamber for organ isolation procedures, catalog No. 166070, Grass Technologies, Monrovia, CA, USA). The isolated kidney was used to employ a recirculating perfusion design by means of an ex vivo perfusion apparatus. The working perfusate, an oxygenated modified Krebs-Henseleit solution (MKHS) at 37°C and aerated with a 19/1 (v/v) mixture of O_2: CO_2 was perfused through the renal artery by means of a recirculating a rotary pump (EYELA, Roller pump, RP-1000). The rabbit IPK was maintained at constant perfusion flow rate (40–60 ml/min), which was carefully kept at 100 mmHg throughout all the experiments.

Preparation of the MKHS in100 ml consisting: 141 mM Na^+, 5.4 mM K^+, 1.9 mM Ca^{2+}, 2.4 mM Mg^{2+}, 126 mM Cl^-, 25 mM HCO_3^-, 2.44 mM SO_4^{2-}, 1.5 mM PO_4^{3-}, and 13 mM amino acids comprised of twenty physiological amino acids (Taft, 2004). The total perfusate also contained 100 mg D-glucose, 50 mg inulin including oncotic agents which was modified in our laboratory by the addition of both 3 g of bovine serum albumin (fraction V, from Sigma Chemical Co., St Louis. MO, USA) and 2 g of dextran (Sigma Chemical Co.). The perfusion solution was adjusted at pH 7.4 and kept warm at 37°C by a pre-warming coil and oxygenation by the addition of a 1.2 μm filter in tissue bath organ chamber. Changes in the perfusion pressure (PP) in the kidney were measured at the tip of the stainless-steel cannula with either a manometer or recorded on a Statham strain gauge pressure transducer, which was modified to allow continuous recorded monitoring the PP on the physiograph (Polygraph Model 79, Grass instruments Co.). The

	Enzyme Specific Activity				Molecular weight
	PLA2	Protease	LAAO	PDE	(kDa)
	(nM/mg)	(uM//mg)	(U/mg)	(U/mg)	
Crude venom	806	0.13	0.02	1.1	
PLA2	2099				13
Proteases		0.33			90
L-amino acid oxidases			40		60
Phosphodiesterase				14.0	110
Purification (fold)	2.6	2.5	200	12.7	
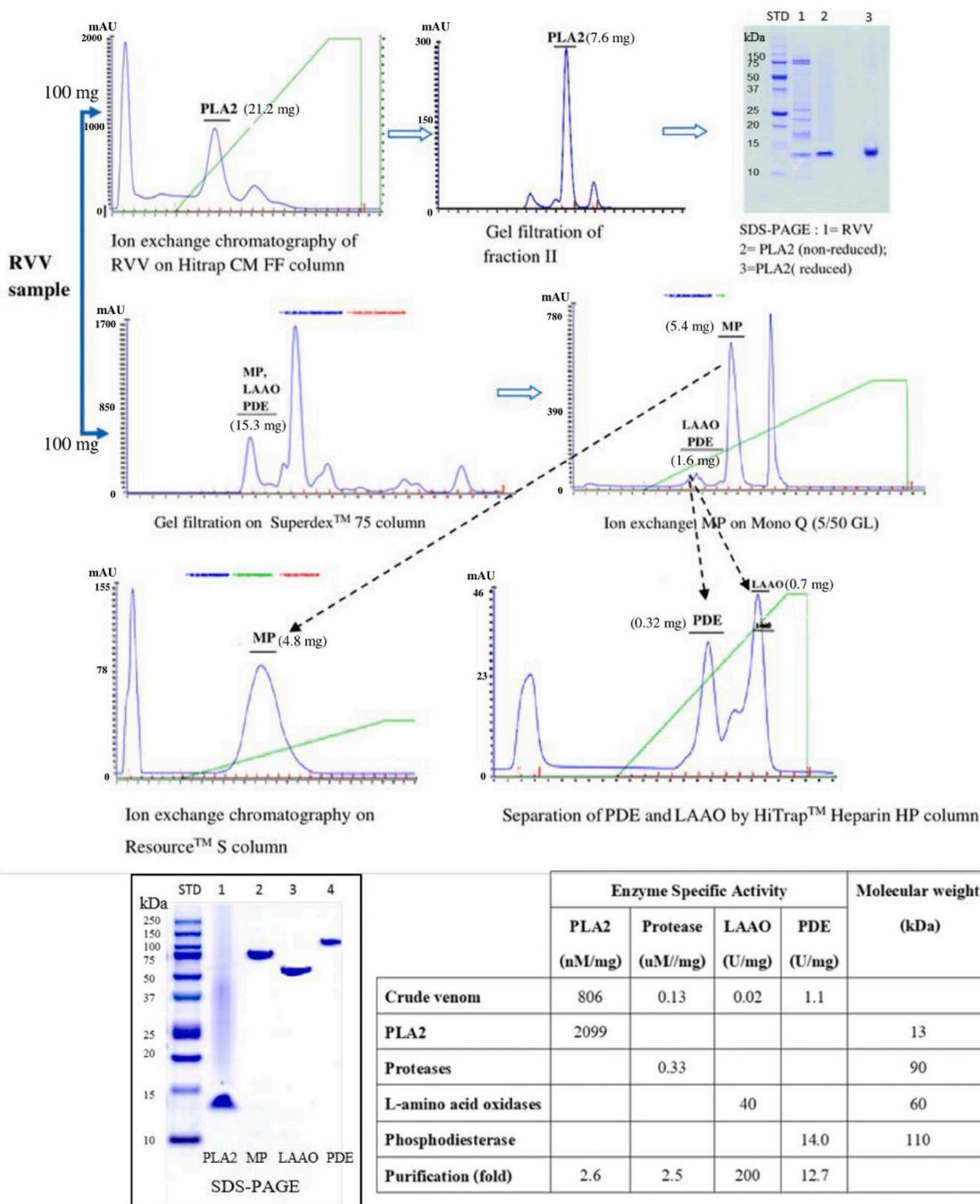
Fig. 1. Schematic representation of the different work flows employed to fractionate the crude RVV. Numbers in parentheses represent the protein yields during fractionation of the crude RVV. For detailed information, please see "Materials and methods".

kidney was mounted in the perfusion system for 30 min to allow the kidney to approach its normal function, as indicated by the maintenance of the urine flow (UF) and PP, which was carefully kept at 100 mmHg. The PP was measured at 5-min intervals after equilibration. The first 30 min of perfusion were considered to be internal control. The experimental period was divided into five intervals of 5, 10, 30, 60, and 90 min of perfusion time. The experiments were conducted over 90 min administration of RVV or one of its fractions administration. In each interval period, samples of perfusate and urine were collected for 5 min for determination of the sodium (Na+), potassium (K+), inulin and osmolality levels.

2.3. Venom and chemicals

A pool of RVV was obtained from 14 adult male and female Russell's viper (*Daboia siamensis*) snakes collected from the eastern region of Thailand and maintained at Queen Saovabha Memorial Institute, The Thai Red Cross Society. The RVV was milked, lyophilized, and stored at $-20\ ^{\circ}C$. The crude RVV (100 mg) was isolated by fractionation methods for phospholipase A_2 (RvPLA$_2$), which gave 7.6 mg of protein yield. Another crude RVV (100 mg) was isolated by fractionation methods for metalloprotease (RvMP), L-amino acid oxidase (RvLAAO) and phosphodiesterase (RvPDE), which gave protein yields 4.8 mg, 0.7 mg and 0.32 mg, respectively, for comparative purposes (Fig. 1). The PAF (β-acetyl-γ-O-alkyl-L-α-phosphatidylcholine), purchased from Sigma-Aldrich, was dissolved in solution of 100 mM DMSO and 100 mM ethanol to give a stock solution of 2000 µg/ml and stored at $-20\ ^{\circ}C$. The triazolobenzodiazepine substance (WEB, 2086) was purchased from Sigma-Aldrich Co. (Saint Louis, MO, USA), and was dissolved in solution of 100 mM DMSO and 100 mM ethanol with gentle warming to give a stock solution of 2 µg/µl and stored at $-20\ ^{\circ}C$. All chemicals were reagent grade.

2.3.1. Isolation of RvPLA$_2$

Crude RVV (100 mg) was dissolved in buffer A (50 mM phosphate buffer pH 6.0). After centrifugation at 7826 g for 5 min, the supernatant was applied to ion-exchange chromatography on HiTrap CMFF column (GE Healthcare, Sweden). The column was washed with five volumes of buffer A and elution was performed with an increasing linear concentration gradient of NaCl from 0 to 1 M in buffer An at a flow rate of 0.5 ml/min. Fractions of 1 ml were collected and measured at an absorbance of 280 nm (A_{280}) under an AKTA pure Fast Protein Liquid Chromatography system (FPLC, GE Healthcare, Sweden). Four peaks were observed and determined for PLA$_2$ activity. Fractions containing PLA$_2$ activity were pooled (21.2 mg protein) and further enriched by size exclusion chromatography in a pre-equilibrated Superdex™ 75 10/300 GL column (GE Healthcare, Sweden). Elution was performed with 10 mM phosphate buffered saline pH 7.4 at room temperature. The flow rate was adjusted to 0.5 ml/min, and 1 ml fractions were collected in each tube. The protein elution and concentration was determined by A_{280} under a Unicorn 6.3 Software.

2.3.1.1. Determination of PLA$_2$ activity.
The PLA$_2$ activity was ascertained as described (Holzer and Mackessy, 1996) with slight modifications. The sample (50 µl) was mixed with 3 mM 4-nitro-3-(octanoyloxy) benzoic acid (Enzo Life Sciences, New York, U.S.A.) at a 1:1 (v/v) ratio and incubated at 37 °C for 20 min. Then 2.5% (v/v) Triton X-100 was added to the reaction mix and the absorbance was measured at 425 nm (A_{425}). A standard curve of A_{425} as a function of chromophore (3-hydroxy-4-nitrobenzoic acid) concentration showed that a change in A_{425} of 0.1 AU was equivalent to 25.8 nmoles of chromophore release.

2.3.2. Isolation of RvMP, RvLAAO, and RvPDE from the crude RVV

The crude RVV (100 mg) was dissolved in buffer A for the isolation of RvMP, RvLAAO, and RvPDE. After centrifugation at 10,000 rpm for 5 min, the supernatant was applied on Superdex™ 75 10/300 GL column equilibrated with 0.1 M sodium acetate buffer pH 6.7 and eluted at a flow rate of 0.4 ml/min, collecting 1 ml fractions under an AKTA pure FPLC system. Each fraction was assayed for enzymatic activity. The active fraction was collected, desalted, and concentrated by centrifugal ultrafiltration (Macrosep® 10K; Pall Corp, UK). The sample was then loaded onto a Mono Q column (5/15 GL; GE healthcare, Sweden) pre-equilibrated with buffer B (50 mM Tris-HCl buffer pH 8.0) and eluted with a 60% linear gradient buffer C (1 M NaCl). Three peaks were separated, the first two active peaks were RvLAAO and RvPDE (1.6 mg protein) and the second active peak was RvMP (5.4 mg protein), which was further enrichedon a Resource S column pre-equilibrated with 10 mM sodium phosphate buffer pH 6.7, and eluted with a linear gradient of 0–0.3 M NaCl.

2.3.2.1. Activity of the RvMP.
The MP activity was determined by estimation of the proteolytic activity by hydrolysis of heated casein, as previously described (Anson, 1938) with slight modifications. The reaction mixture consisted of 500 µl casein in 0.1 Tris-HCl pH 8.0 and 50 µl of venom, and was incubated for 2 h at 37 °C. The reaction was quenched by the addition of 500 µl of 5% (w/v) trichloroacetic acid at room temperature. After centrifugation, the supernatant (400 µl) was mixed with 1 ml of 0.5 M Na$_2$CO$_3$ and 200 µl of diluted (1:5) Folin & Ciocalteau's phenol reagent. The mixture was then incubated at 37 °C for 30 min and the absorbance was measured at 660 nm (A_{660}). One enzyme U was defined as the amount of enzyme that hydrolyzes casein to produce a color equivalent to 1.0 µmole of tyrosine per min. The effect of the protease inhibitor on the proteolytic activity of the sample was observed by pre-incubated the sample with EDTA (final concentration of 10 mM) at 37 °C for 10 min. The mixture was then assayed for MP activity in the corresponding assay systems.

2.3.3. Isolation of RvPDE and RvLAAO
After the supernatant of crude RVV was fractionated on Superdex™ 75 10/300 GL column, the active fraction was collected and the sample was then applied on a Mono Q column (5/15 GL; GE healthcare, Sweden). The first peak (1.6 mg protein) from the Mono Q column, which expressed PDE and LAAO activities, was further enriched by a HiTrap™ Heparin HP column (GE Healthcare, Sweden) pre-equilibrated with 50 mM Tris-HCl pH 8.0 and eluted with a linear gradient of 0–0.5 M NaCl (Fig. 1).

2.3.3.1. Determination of RvLAAO activity.
The RvLAAO activity was determined according to the Worthington Enzyme Manual (1977). A reaction mixture (510 µl) containing 0.1% (w/v) L-leucine, 0.0065% (w/v) o-dianisidine, and 0.007% horse radish peroxidase in 0.2 M Triethanolamine buffer pH 7.6 was incubated at 37 °C. The reaction was started by adding the respective LAAO fractions and monitored at 426 nm over 3 min.

2.3.3.2. Determination of RvPDE activity.
The RvPDE activity was determined as previously described (Lo et al., 1966) with slight modifications using Ca-bis-p-nitrophenylphosphate as the substrate. The hydrolysis of the substrate was assessed by measuring the rate of increase in absorbance at 440 nm (A_{440}). One U of enzyme activity was defined as the amount of enzyme that caused an increase of 0.001 A_{440} per min.

2.4. Experimental design

Two experimental protocols were carried out:

2.4.1. Experiment protocol 1
This study was assigned to demonstrate the functional properties of PAF, and whether the effectiveness of PAF were specific and receptor-

mediated on the renal functions in the rabbit IPK. The PAF receptor antagonist, WEB 2086, was used as a blocker to test if effects during exogenous PAF administration in the rabbit IPK were due to PAF. Preparations of IPK were divided into the following six groups (n = 4/ group):

Control group: Following kidney excision and transfer to the recirculating perfusion system, control perfusions were conducted to establish the viability of the preparation and to allow for the evaluation of any agents tested for effects on the kidney function. The rabbit IPK was perfused with MKHS in the absence of any treatment agents in the recirculating system for 120 min.

WEB 2086 group: The 100 μl of WEB 2086 (2 μg/μl) was added the recirculating system in 100 ml of perfusate after the first 30-min equilibration period as an internal control with stabilization of the basal PP.

PAF-L group: After the 30-min equilibration of the internal control period of perfusion, the rabbit IPK was treated with 25 μl of exogenous PAF (200 μg/ml), added into 100 ml of perfusate of the recirculating system. This dose was arbitrarily chosen as a low PAF administration dose with a total PAF concentration in the perfusate of 95 nM.

WEB2086 + PAF-L group: To test if WEB 2086 could block the action of the exogenous PAF-L dose in the IPK model. For this interaction study, 100 μl of WEB 2086 (2 μg/μl) was injected at the start of the perfusion, after the equilibration period, and then 25 μl of PAF (200 μg/ml) was injected 30 min later to the perfusate under the same protocol.

PAF-H group: After the 30-min equilibration of the internal control perfusion, the IPK was treated with 75 μl of exogenous PAF (200 μg/ml), added into 100 ml of perfusate of the recirculating system. This dose was arbitrarily chosen as a high PAF administration dose with a total PAF concentration in the perfusate of 270 nM.

WEB 2086 + PAF-H group: To ascertain whether WEB 2086 could block the action of the exogenous PAF-H dose in the IPK study. For this, 100 μl of WEB 2086 (2 μg/μl) was injected at the beginning of the perfusion and equilibration period, and then after the 30-min pretreatment 75 μl of PAF (200 μg/ml) was injected to the perfusate under the same protocol.

For all six groups, the changes in renal functions were recorded thereafter for a 90-min period (from 30 to 120 min after the initial IPK perfusion).

2.4.2. Experiment protocol 2

The experiment in protocol 2 was assigned to study the effects of RVV and its fractions (RvPLA$_2$, RvMP, RvLAAO, and RvPDE) on the renal functions in the rabbit IPK model, and the potential role of PAF in these effects using the WEB 2086 PAF receptor inhibitor. Preparations of rabbit IPK were divided into 10 experimental groups (n = 4/group) as follows:

RVV group: The rabbit IPK was treated with 1 ml of the lyophilized RVV in normal saline (1 mg/ml), added into 100 ml of perfusate of the recirculating system after the 30-min equilibration period as an internal control. This dose was arbitrarily chosen on the basis of an earlier investigation in experimental animals in either dogs or rabbits, where the dosage of crude RVV that caused death in 50% of subjects (LD$_{50}$) by intravenously injection was 0.5 mg/kg body weight (BW) (Chaiyabutr et al., 2014; Tungthanathanich et al., 1986). This dosage was equivalent to a concentration of 10 μg/ml plasma, based upon an estimated plasma volume of 5% of the BW. For this, 1 mg of RVV was added to 100 ml of perfusate to obtain a final concentration of 10 μg/ml.

WEB 2086 +RVV group: The rabbit IPK was pretreated with 100 μl of WEB 2086 (2 μg/μl) after the 30-min equilibration period and then after this 30-min pretreatment period 1 ml of RVV (1 mg/ml) was added into 100 ml of perfusate of the recirculating system.

PLA$_2$ group: The rabbit IPK was treated with 1 ml of the RvPLA$_2$ fraction (280 μg/ml), added into 100 ml of perfusate of the recirculating system after the 30-min equilibration period as an internal control. This dose was arbitrarily chosen and adjusted according to that previously described (Mitrmoonpitak et al., 2013) using a PLA$_2$ dose of 140 μg/kg

BW by intravenous injection, which converted to 2.8 μg/ml plasma using the estimated plasma volume of 5% of the BW. Therefore, the amount of RvPLA$_2$ used in the present study was adjusted by adding 280 μg RvPLA$_2$ into 100 ml of perfusate.

WEB 2086 +PLA$_2$ group: The rabbit IPK was pretreated with 100 μl of WEB 2086 (2 μg/μl) after the 30-min equilibration perfusion. Then, 1 ml of the RvPLA$_2$ (280 μg/ml) was added to the recirculating solution after the 30-min pretreatment period.

MP group: The rabbit IPK was treated with 1 ml of the RvMP fraction (280 μg/ml), added into 100 ml perfusate of the recirculating system after the 30-min equilibration period as an internal control. This dose was arbitrarily chosen and adjusted according to the previously described work (Mitrmoonpitak et al., 2013) that used a MP dose of 140 μg/kg BW by intravenously injection. This dosage converted to 2.8 μg/ml plasma, based upon the estimated plasma volume of 5% of the BW (adding 280 μg RvMP into 100 ml of perfusate).

WEB 2086 + MP group: The rabbit IPK was pretreated with 100 μl of WEB 2086 (2 μg/μl) after the 30-min equilibration perfusion. After the 30-min WEB 2086 pretreatment, 1 ml of RvMP (280 μg/ml) was added to the recirculating solution.

LAAO group: The rabbit IPK was treated with 2 ml of RvLAAO (135 μg/ml), added into 100 ml of perfusate of the recirculating system after the 30-min equilibration period, as an internal control. This dose was arbitrarily chosen for comparison with the other venom fractions, where 270 μg RvLAAO was added into 100 ml of perfusate.

WEB 2086 + LAAO group: The rabbit IPK was pretreated with 100 μl of WEB 2086 (2 μg/μl) after the 30-min equilibration perfusion. After the 30-min WEB 2086 pretreatment, 2 ml of RvLAAO (135 μg/ml) was added to the recirculating solution.

PDE group: The rabbit IPK was treated with 2 ml of RvPDE (100 μg/ ml), added into 100 ml perfusate of the recirculating system after the 30-min equilibration period, as an internal control. This dose was arbitrarily chosen for comparison with the other venom fractions, where 200 μg RvPDE was added in 100 ml of perfusate.

WEB 2086 + PDE group: The rabbit IPK was pretreated with 100 μl of WEB 2086 (2 μg/μl) after the 30-min equilibration perfusion. After the 30-min WEB 2086 pretreatment, 2 ml of RvPDE (100 μg/ml) was added to 100 ml of the recirculating solution.

In all ten groups, the changes in renal functions were recorded thereafter for a 90-min. Period after addition of the final treatment (from 5,10, 30,60 or 90 min–120 min).

2.5. Samples collection and chemical analysis

Each experimental group was divided into six periods for renal function measurements after each specified treatment. Samples of urine and perfusate were collected at 5-min intervals of each specified period (at 0, 5, 10, 30, 60, and 90 min after treatment) for analysis of the Na$^+$, K$^+$, inulin, osmolality, and urinary NO levels. The Na$^+$ and K$^+$ ion concentrations were determined by flame photometer (Flame Photometers, Laboratory Instrument, BWB Technologies UK Ltd), while the osmolality was measured using an osmometer (Fiske® Micro-osmometer Model210, Fiske® Associates, Norwood, Massachusetts, 02062, USA). The inulin concentration in both the perfusate and urine was determined using the anthrone method (Young and Raisz, 1952).

Urine samples, stored at −40 °C until used, were determined for the NO concentration. Nitrite and nitrate are the primary oxidation products of NO and, therefore, the nitrite/nitrate concentration in urine was used as an indicator of NO release. The NO levels were quantified using an Arrowstraight™ Nitric Oxide measurement system (Lazar Research Laboratories, Los Angeles, CA, USA), which contained -on selective electrodes for independent measures of both nitrite and nitrate in each 100-μl urine sample. As a standard, known sodium nitrite and sodium nitrate concentrationswere used (Sigma-Aldrich, Natick, MA, USA; for both). All procedures were conducted according to the manufacturer's protocol. Results are presented as the total NO (μM) calculated by

summing the concentration values of nitrite and nitrate.

2.6. Histological studies of the rabbit IPK

The control and treated kidneys were cut sagittally after termination of the 120-min perfusion period and preserved in 10% (v/v) neutral buffered formalin (v/v) for 24 h before dehydration using increasing alcohol concentration gradients and paraffin embedding in paraffin blocks. The kidney tissues were then cut into 4-μm thick serial sections and subsequentially stained with routine Hematoxylin and Eosin (H&E) or periodic acid-Schiff reaction (PAS) for morphological studies. Histological examinations were performed under a light microscope (Olympus, Tokyo, Japan) for the H&E− and PAS-stained sections, which were used to assess changes in the glomerulus, proximal and distal convoluted tubules, and collecting duct of the IPK. Each section was examined, for at least 50 glomeruli and 10 area of tubules, from one section per kidney. Effects of the RVV, RvPLA₂, RvMP, RvLAAO, RvPDE, and WEB 2086 on the changes in the glomeruli and renal tubules were assessed. The level of histopathological lesions was quantitated by scoring from 0 to 3+ (0, no lesion; 1+, mild lesion; 2+, moderate lesion; 3+, marked lesion). Glomerular congestion and crystal deposits in the glomerulus, and the renal tubular changes (tubulonephrosis and tubule-necrosis, in the proximal tubule, distal tubule, and collecting tubule) were all graded separaretely from 0 to 3+ (0, no changes; 1+, mild

changes; 2+, moderate changes; 3+, marked changes of sample).

2.7. Calculations for renal function

The PP, renal vascular resistance (RVR), UF, GFR, and the fractional sodium (%FENa⁺) and potassium (%FEK⁺) tubular excretions were determined as described previously (Chaiyabutr et al., 2014). The experimental results were compared with those of the internal control at 30 min in each group. The clearance of inulin (Cin, GFR) and osmolality (Cosm) were calculated according to the standard formula (Smith, 1962). The flow rate of the perfusate to the kidney and the PP of the system were used to calculate for the RVR, using the standard formula (PP/perfusate flow rate). The %FENa⁺ and %FEK⁺ were calculated by dividing the CNa⁺ or CK⁺ with GFR, respectively.

2.8. Statistical analysis

The results are expressed as mean ± one standard deviation (SD). One-way repeated measures ANOVA was used with Bonferroni's post-hoc test to compare the number of changes among time points after each agent treatment within the same group. At each agent treatment, the data of pretreatment with WEB2086 group were compared with corresponding untreated group using unpaired Student's t-test at some time points. Significance was accepted at the $P < 0.05$ level. All data
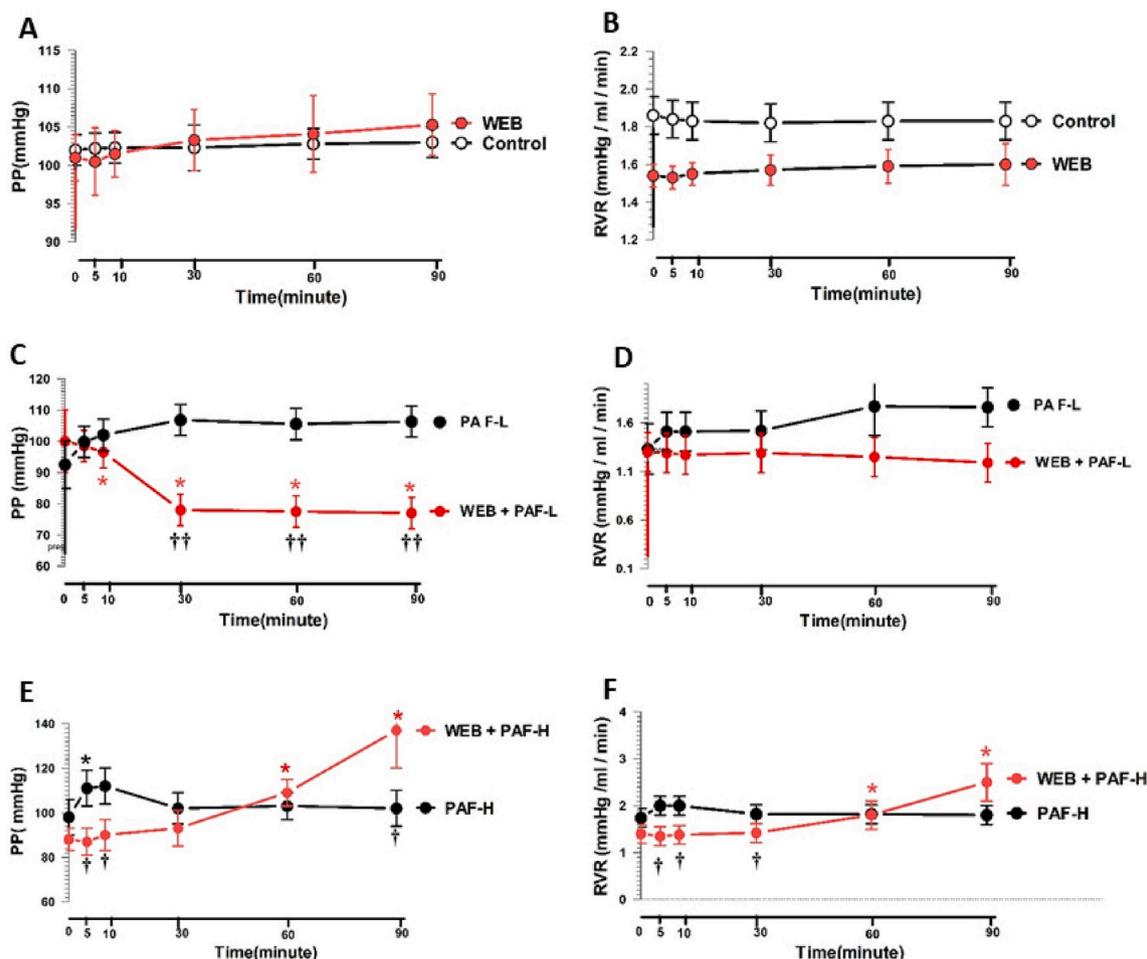
Fig. 2. Changes in the PP and RVR at various time points in response to a low (PAF-L) or high (PAF-H) exogenous PAF dosage with or without WEB 2086 pretreatment in the rabbit IPK. Comparison between groups treated with MKHS (Control) and WEB 2086 (WEB) (A and B); PAF-L without (PAF-L) and with WEB 2086 pretreatment(WEB + PAF-L) (C and D); PAF-H without (PAF-H) and with WEB 2086 pretreatment(WEB + PAF-L) (E and F). Data are shown as the mean ± SD of four experimental kidneys. *Significant difference ($P < 0.05$; repeated measures ANOVA with Bonferroni post-hoc test between the specified time point and the internal control in the same group. Comparisons between two sets of data at each specified time point between the treated group without WEB 2086 pretreatment and with WEB 2086 are shown by †P < 0.05 and ††P < 0.01 (unpaired Student's t-test).

were analyzed by GraphPad Prism 5 for Windows (GraphPad Software, San Diego, CA, USA).

3. Results

3.1. Effects of exogenous PAF and WEB 2086 administration on the renal functions in IPK

Under experimental protocol 1, in the control conditions, the IPKs were preserved functionally, as seen in the data shown in Figs. 2–5. The renal hemodynamics, glomerular filtration function, tubular Na^+ and K^+ transport, and Cosm parameters were stable after perfusion with MKHS alone for over 120 min. In comparison with the control group, when WEB 2086 at 2 µg/µL was administered, the kidney functional parameters remained stable throughout the perfusion time (Figs. 2–4A, B; Fig. 5A).

Increasing the PAF availability by adding the concentration of PAF alone into the perfusate at either PAF-L (95 nM) or PAF-H (270 nM) caused an increase in the PP and RVR throughout the 90-min perfusion time (Fig. 2C–F). Pretreatment with WEB 2086 significantly decreased the PAF-L-mediated increase in the PP throughout the 90-min perfusion time, decreasing from 121.8 ± 12.5 to 77.0 ± 10.1 mmHg (P < 0.05) but RVR slightly decreased as shown in Fig. 2C and D. However, the increase in both PP and RVR induced by PAF-H was not completely prevented by

WEB 2086 pretreatment, as there were still significant increases in both the PP and RVR at 60 min (p < 0.05) and 90 min (p < 0.05) of perfusion time compared to the pretreated period (Fig. 2E and F).

The effect of exogenous PAF on the GFR and UF in the rabbit IPK is shown in Fig. 3. The administration of PAF-L caused a slight reduction in the GFR throughout the perfusion time, while the UF showed a transient reduction in the first 10 min followed by significant increase after 60 min of perfusion (P < 0.05) with a maximal response at 90 min (P < 0.05) compared to the control period. Pretreatment with WEB 2086 (2 µg/µl) abrogated the PAF-L effect on the UF but not the GFR (Fig. 3C and D). The high PAF dose increased the GFR and UF throughout the perfusion time, but these effects were abolished by WEB 2086 (2 µg/µl) pretreatment (Fig. 3E and F), and prevented the effect of PAF-L on further increasing the UF at 30 and 90 min of perfusion time.

The administration of either PAF-L or PAF-H alone caused a small initial decrease in the %FENa$^+$, %FEK$^+$, and Cosm at 5 min after administration, and further increases were apparent throughout the perfusion time. A significantly increased %FENa$^+$, with a maximal response at 60 min (P < 0.05), was apparent after administration of PAF-H and pretreatment with WEB 2086 significantly abolished the PAF-H effects on the %FENa$^+$ (P < 0.05) and Cosm, but not the effect on the %FEK$^+$ (Fig. 4E and F and Fig. 5C). Pretreatment with WEB 2086 prevented the PAF-L effects on Cosm with a maximal effect at 90 min (P < 0.05), but did not prevent the changes in the %FENa$^+$ and %FEK$^+$ when
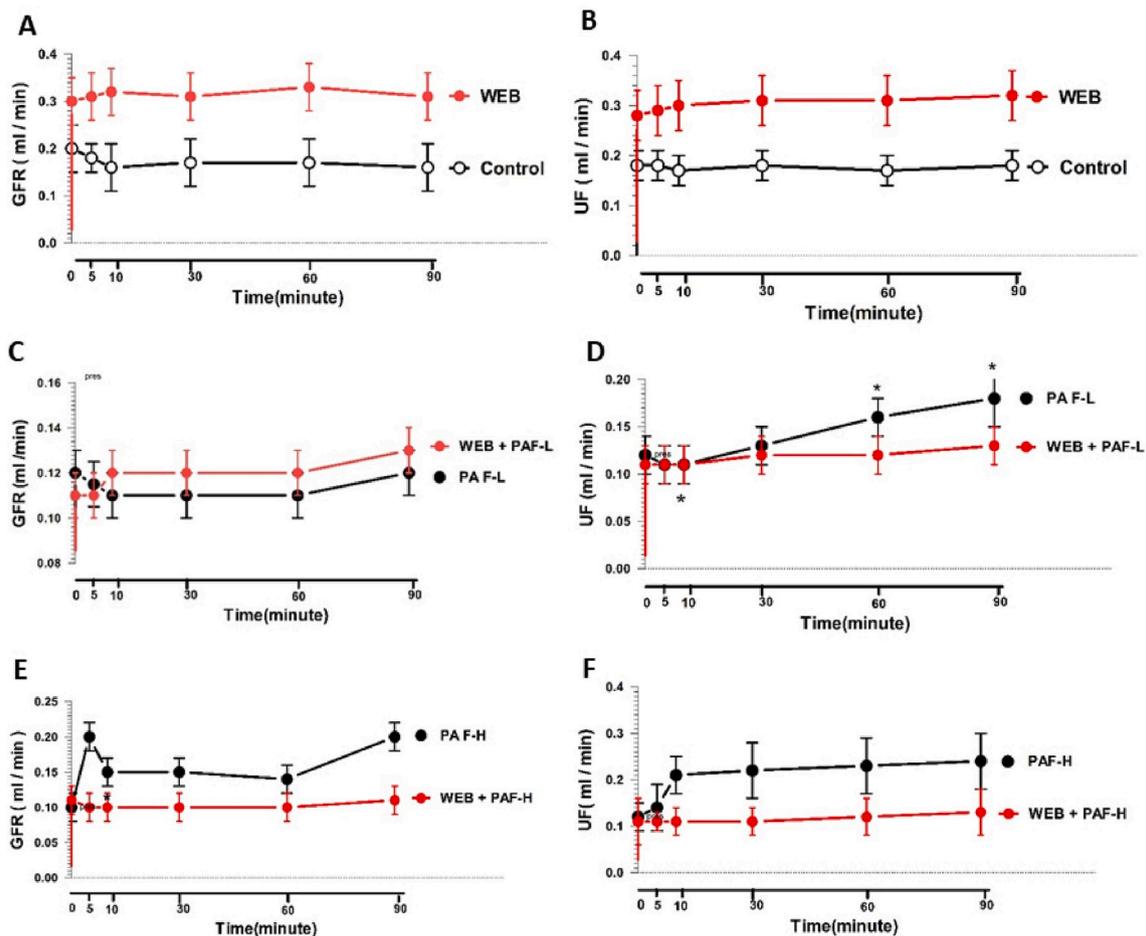
Fig. 3. Changes in the mean GFR and UF at various time points in response to a low (PAF-L) or high (PAF-H) exogenous PAFdose with or without WEB 2086 pretreatment in the rabbit IPK. Comparison between groups treated with MKHS (Control) and WEB 2086 (WEB) (A and B); PAF-L without (PAF-L) and with WEB 2086 pretreatment(WEB + PAF-L) (C and D); PAF-H without (PAF-H) and with WEB 2086 pretreatment(WEB + PAF-L) (E and F). Data are shown as the mean ± SD of four experimental kidneys. *Significant difference (P < 0. 05; repeated measures ANOVA with Bonferroni post-hoc test between the specified time point and the internal control in the same group. Comparisons between two sets of data at each specified time point between the treated group without WEB 2086 pretreatment and with WEB 2086 are shown by †P < 0.05 (unpaired Student's t-test).

Fig. 4. Changes in the %FENa⁺ and %FEK⁺ at various time points in response to a low (PAF-L) or a high (PAF-H) exogenous PAFdose with or without WEB 2806 pretreatment in the rabbit IPK. Comparison between groups treated with MKHS (Control) and WEB 2086 (WEB) (A and B); PAF-L without (PAF-L) and with WEB 2086 pretreatment(WEB + PAF-L) (C and D); PAF-H without (PAF-H) and with WEB 2086 pretreatment(WEB + PAF-L) (E and F). Data are shown as the mean $\pm$ SD of four experimental kidneys. *Significant difference ($P < 0.05$; repeated measures ANOVA with Bonferroni post-hoc test between the specified time point and the internal control in the same group. Comparisons between two sets of data at each specified time point between the treated group without WEB 2086 pretreatment and with WEB 2086 are shown by †P < 0.05 (unpaired Student's t-test).

compared to the effect observed with PAF-L alone (Fig. 4C and D and Fig. 5B).

3.2. Effects of RVV, RvPLA₂, RvMP, RvLAAO, RvPDE, and WEB 2086 on the rabbit IPK renal hemodynamics

During administration of whole RVV alone (1 mg/ml), the biphasic responses of renal hemodynamics were apparent. Significant initial decreases ($P < 0.05$) in the PP and RVR occurred in the first phase compared to the basal level of the internal control. This effect was transient and occurred for 5–10 min after administration of RVV. A gradual rise in both the PP and RVR occurred from 10 min after the initial transient reduction, but the values remained below the pretreatment values throughout the experimental period. These effects were abolished by WEB 2086 pretreatment, with a reversal in the marked fall in PP and RVR ($P < 0.05$) throughout the perfusion time (Fig. 6A and B). Administration of RvPLA₂, RvMP, RvLAAO, and RvPDE on the renal hemodynamics showed some differences. Administration of RvPLA₂ (280 µg/ml) caused a significant increase in the PP and RVR ($P < 0.05$) with a maximal effect at 60 and 90 min of perfusion, and these effects were not prevented by WEB 2086 pretreatment (Fig. 6C and D). Administration of RvMP (280 µg/ml) also caused a significant increase in the PP and RVR ($P < 0.05$) at 60 and 90 min of perfusion time, but

these effects were abolished by pretreatment with WEB 2086 with significant differences of PP were apparent from 30 to 90 min ($P < 0.01$) (Fig. 6E and F).

Administration of RvLAAO (135 µg/ml) and RvPDE (100 µg/ml) alone slightly increased and decreased, respectively, the PP and RVR levels compared with the basal control levels, and these effects were not prevented by pretreatment with WEB 2086 (Fig. 6G–J).

3.3. Effects of RVV, (RvPLA₂, RvMP, RvLAAO, RvPDE, and WEB 2086 on the GFR and UF

The present study demonstrated that administration of RVV caused a significant decrease in both the GFR and UF with significant reductions ($P < 0.05$) observed at 60 and 90 min of perfusion, and were not abrogated by pretreatment with WEB 2086 (Fig. 7A and B). In contrast to RVV, administration of RvPLA₂, RvMP, RvLAAO, and RvPDE alone each increased the GFR and UF thoughout the perfusion time, which was significant for both the GFR and UF (P < 0.05), especially in RvPLA₂ and RvMP after 60 and 90 min of perfusion. These effects by RvPLA₂ and RvMP were abolished by pretreatment with WEB 2086 (Fig. 7C–F), but not those induced by RvLAAO or RvPDE (Fig. 7G–J).
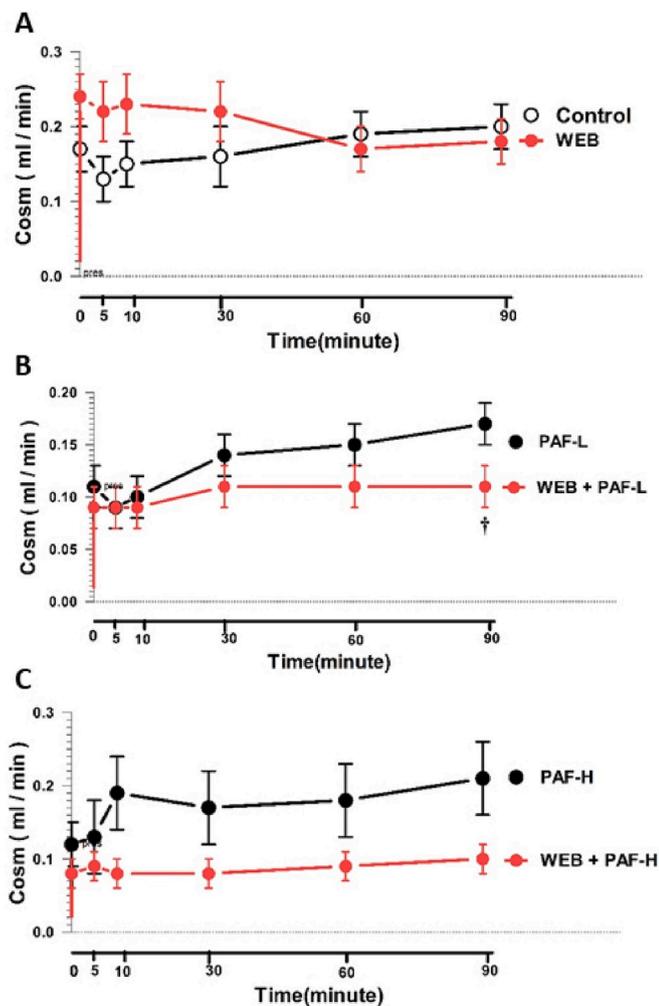
Fig. 5. Changes in the Cosm at various time points in response to a low (PAF-L) or a high (PAF-H) exogenous PAF dose with or without WEB 2806 pretreatment in the rabbit IPK. Comparison between groups treated with (A) MKHS (Control) and WEB 2086 (WEB); (B) PAF-L without (PAF-L) and with WEB 2086 pretreatment(WEB + PAF-L); (C) PAF-H without (PAF-H) and with WEB 2086 pretreatment(WEB + PAF-L). Data are shown as the mean ± SD of four experimental kidneys. *Significant difference ($P < 0.05$; repeated measures ANOVA with Bonferroni post-hoc test between the specified time point and the internal control in the same group. Comparisons between two sets of data at each specified time point between the treated group without WEB 2086 pretreatment and with WEB 2086 are shown by †P < 0.05 (unpaired Student's t-test).

3.4. Effects of RVV, RvPLA$_2$, RvMP, RvLAAO, RvPDE, and WEB 2086 on the %FENa$^+$ and %FEK$^+$

The %FENa$^+$ increased after administration of RVV, with a maximal effect after 90 min of perfusion (P < 0.05) while the %FEK$^+$ showed a tendency to increase but was not statistically significant and these effects were abolished by pretreatment with WEB 2086 (Fig. 8A and B).

The administration of RvPLA$_2$ or RvMP showed different responses on the renal tubular transport of Na$^+$ and K$^+$ compared to that with RVV. Administration of RvPLA$_2$ alone showed a tendency to decrease either the %FENa$^+$ or the %FEK$^+$ throughout the perfusion time, whereas marked increases in the %FENa$^+$ (P < 0.05) were induced by RvPLA$_2$ following pretreatment with WEB 2086, but this was not apparent for the %FEK$^+$ throughout the perfusion time (Fig. 8C and D).

The effect of RvMP was to induce a slight decrease in the %FENa$^+$, while the %FEK$^+$ significantly decreased (P < 0.05) with sustained

reductions being apparent throughout the perfusion time. These effects were prevented by WEB 2086 pretreatment (Fig. 8E and F). The administration of RvLAAO increased the %FENa$^+$ with a maximal effect at 10 min after administration ($P < 0.05$), while the %FEK$^+$ showed a further decrease throughout the perfusion time, and these effects were not abolished by WEB 2086 pretreatment (Fig. 8G and H). The administration of RvPDE alone caused a significant increase ($P < 0.05$) in both the %FENa$^+$ and %FEK$^+$ with a maximal effect after 30 min of perfusion time ($P < 0.05$), which was abolished by WEB 2086 pretreatment (Fig. 8I and J).

3.5. Effects of RVV, RvPLA$_2$, RvMP, RvLAAO, RvPDE, and WEB 2086 on the renal cosm and urinary NO level

The administration of RVV caused a significant reduction ($P < 0.05$) in the Cosm at 60 and 90 min of perfusion that was not prevented by pretreatment with WEB 2086 (Fig. 9A). The venom fractions RvPLA$_2$, RvMP, RvLAAO, and RvPDE alone caused significant increases ($P < 0.05$) in the Cosm throughout the perfusion time, and these effects were prevented by WEB 2086 pretreatment (Fig. 9B–E).

The NO formation in the rabbit IPK was measured in terms of the urinary nitrate plus nitrite (NOx) concentrations taken in each experimental period. No significant alterations in the NO concentration in urine were apparent in the control or any of the treatments (Table 1).

3.6. Effects of RVV, RvPLA$_2$, RvMP, RvLAAO, RvPDE, and WEB 2086 on kidney histological alterations

Light microscopy of the rabbit IPK perfused with MKHS alone (control group) revealed a normal renal parenchyma in both the glomerular and tubular parts (Fig. 10A–D). The rabbit IPK perfused with WEB 2086 also showed no remarkable lesions in both the glomerular and tubular parts, except for a dilated lumen of the proximal and distal tubule (Fig. 10E–H). A normal brush border was apparent in the proximal convoluted tubule with PAS staining in both the control and WEB 2086 treated rabbit IPK (Fig. 10C, D, G, H).

The sections from the rabbit IPK taken after 90 min of administration with whole RVV produced no remarkable lesions in the glomerular parts, while the proximal and distal convoluted tubules revealed dilatation and moderate tubulonephrosis (+2), and the collecting duct revealed severe tubulonephrosis (+3) (Fig. 11A–D). However, pretreatment with WEB 2086 (WEB, 2086 + RVV) showed no remarkable lesions in the glomerular part, but the proximal and distal convoluted tubules revealed dilatation and mild tubulonephrosis (+1), and the collecting duct had mild tubulonephrosis (+1) (Fig. 11 E–H). However, no distinct brush border was apparent in the proximal convoluted tubules in the rabbit IPK treated with RVV without (Fig. 11D) or with (Fig. 11H) WEB 2806 pretreatment.

Administration of RvPLA$_2$ showed some glomeruli with severe unidentified crystals deposited in the glomerular capillary lumen. The proximal and distal convoluted tubules revealed dilatation and moderate tubulonephrosis (+3), while the collecting duct had moderate tubulonephrosis (+2) (Fig. 12A–D). Pretreatment with WEB 2086 before RvPLA$_2$ showed no remarkable lesions in the glomerular part but the proximal and distal convoluted tubules revealed dilatation and severe tubulonephrosis (+3), while the collecting duct had severe tubulonephrosis (+3) (Fig. 12E–H).

Administration of RvMP showed some glomeruli with severe unidentified crystal deposits in the glomerular capillary lumen, while the proximal and distal convoluted tubules revealed dilatation and severe tubulonephrosis (+3) and the collecting duct had severe tubulonephrosis (+3) (Fig. 13A–D). Administration of RvMP after WEB 2086 pretreatment showed no remarkable lesions in the glomerular part. Some glomeruli showed mild protein deposition in the glomerular capillary lumen, while the proximal and distal convoluted tubules revealed dilatation and severe tubulonephrosis (+3) and the collecting duct had
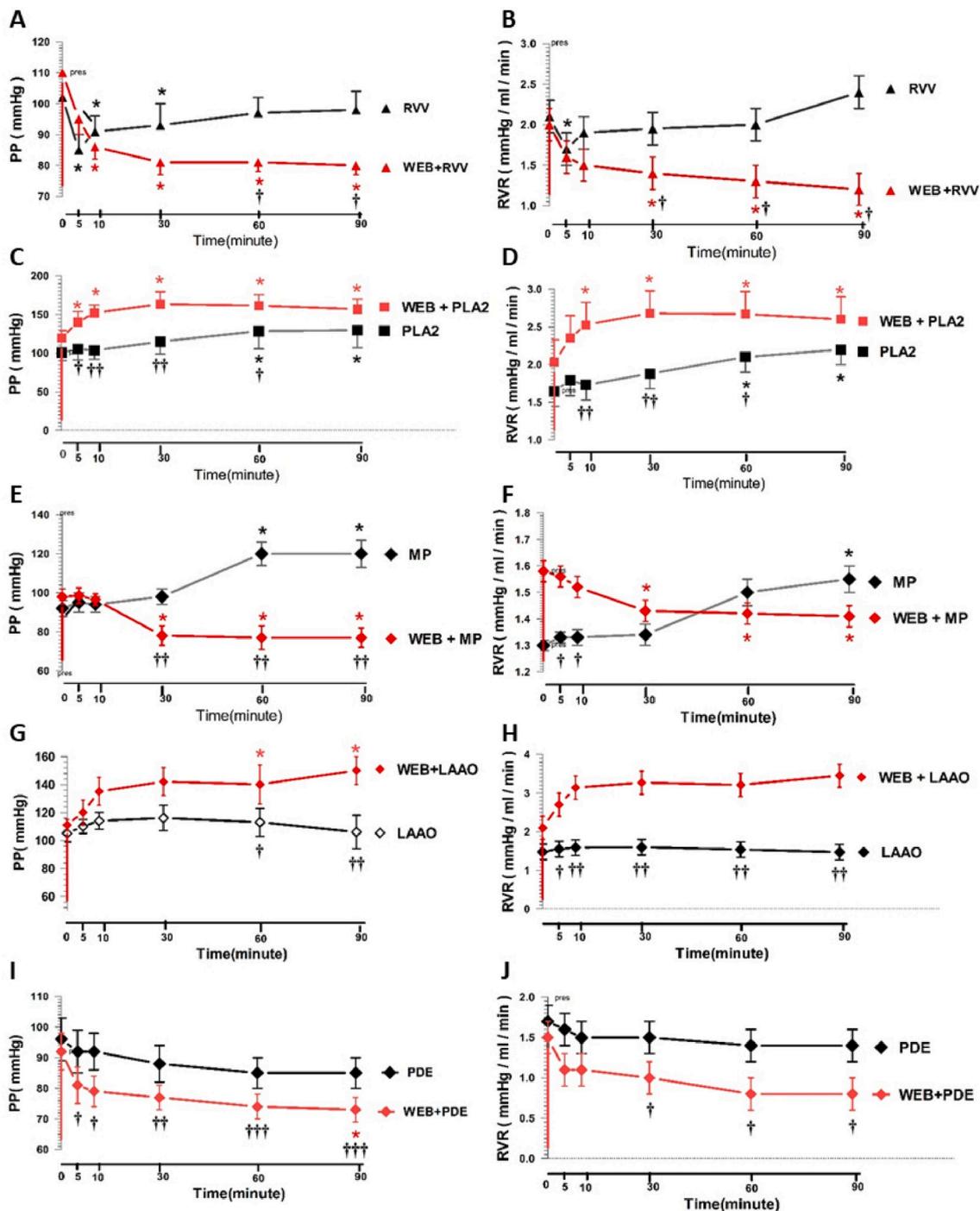
Fig. 6. Changes in the mean renal PP and RVR in response to RVV or its fractions with or without WEB 2086 pretreatment in the rabbit IPK. Comparison between groups treated with or without WEB 2806 pretreatment for RVV(A, B), RvPLA$_2$(C, D), RvMP(E, F), RvLAAO(G, H), and RvPDE(I, J). Data are shown as the mean ± SD of four experimental kidneys. *Significant difference ($P < 0.05$; repeated measures ANOVA with Bonferroni post-hoc test between the specified time point and the internal control in the same group. Comparisons between two sets of data at each specified time point between the treated group without WEB 2086 pretreatment and with WEB 2086 are shown by †$P < 0.05$, ††$P < 0.01$, and †††$P < 0.001$ (unpaired Student's t-test).

severe tubulonephrosis (+3) (Fig. 13E–H).

For the IPK treated with RvLAAO, microscopic findings showed unidentified crystals that appeared to be deposited in the capillary lumen of some glomeruli (Fig. 14A, C). The proximal and distal convoluted tubules revealed dilatation and severe (+3) tubulonephrosis and the collecting ducts had severe (+3) tubulonephrosis (Fig. 14B, D). Pretreatment with WEB 2086 before RvLAAO showed no remarkable lesions in the glomerular part and some mild protein deposition in the capillary lumen of some glomeruliir. The proximal and distal convoluted

tubules still appeared dilated with severe (+3) tubulonephrosis and the collecting ducts had severe (+3) tubulonephrosis (Fig. 14E–H).

The rabbit IPK treated with RvPDE showed severe deposits of unidentified crystals in the capillary lumen of some glomeruli (Fig. 15A, C). The proximal and distal convoluted tubules revealed dilatation and severe (+3) tubulonephrosis, while the collecting ducts had severe (+3) tubulonephrosis (Fig. 15B, D). Pretreatment with WEB 2086 prior to RvPDE showed no remarkable lesions in the glomerular part. Some glomeruli showed mild protein deposition in the glomerular capillary
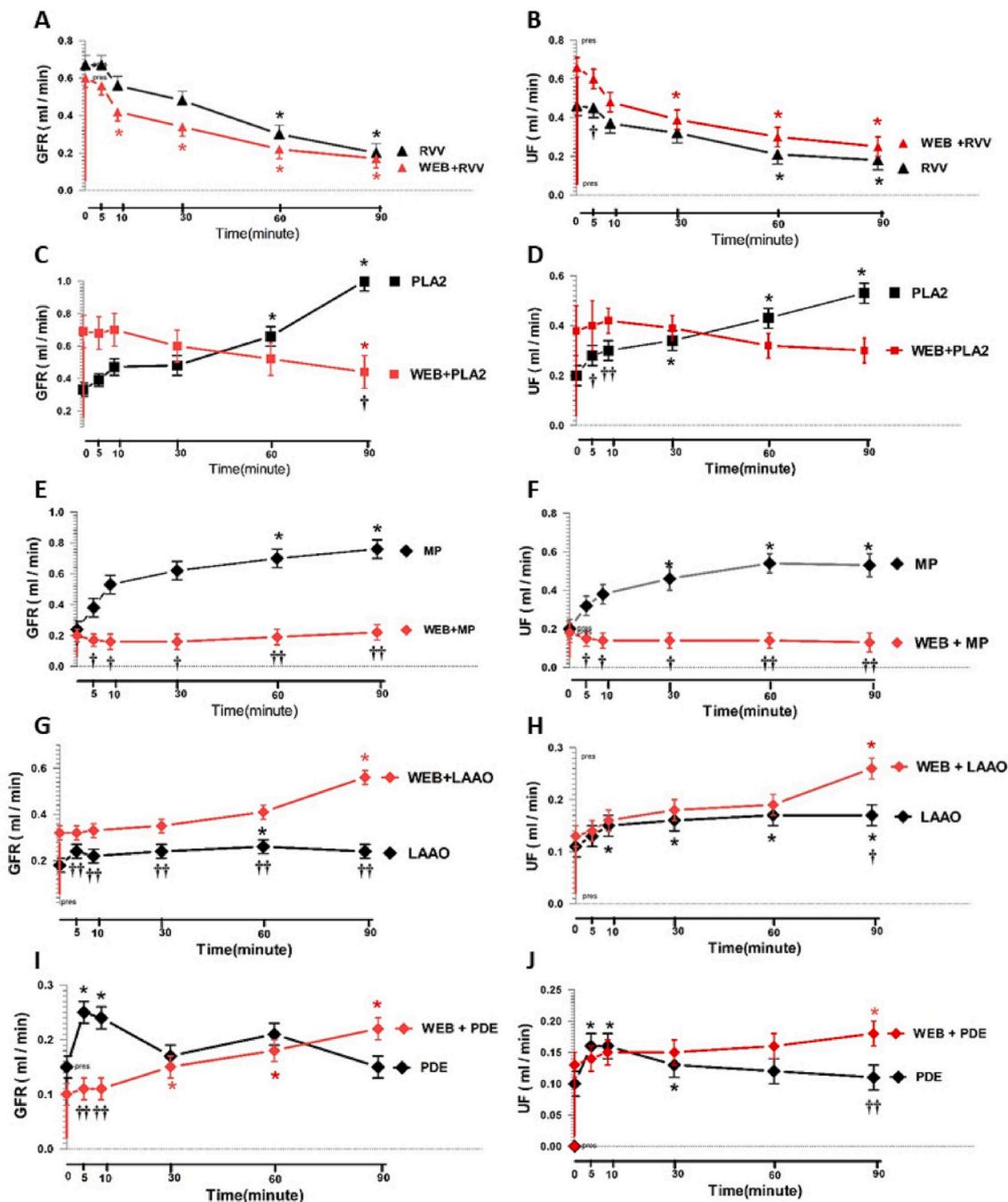
Fig. 7. Changes in the mean GFR and UF in response to RVV or its fractions with or without WEB 2086 pretreatment in the rabbit IPK. Comparison between groups treated with or without WEB 2806 pretreatment for RVV (A, B), RvPLA₂(C, D), RvMP (E, F), RvLAAO(G, H), and RvPDE(I, J). Data are shown as the mean ± SD of four experimental kidneys. *Significant difference (P < 0. 05; repeated measures ANOVA with Bonferroni post-hoc test between the specified time point and the internal control in the same group. Comparisons between two sets of data at each specified time point between the treated group without WEB 2086 pretreatment and with WEB 2086 are shown by †P < 0.05 and ††P < 0.01 (unpaired Student's t-test).

lumen and the proximal and distal convoluted tubules revealed dilatation and severe (+3) tubulonephrosis, while the collecting ducts had severe (+3) tubulonephrosis (Fig. 15F, H).

4. Discussion

The work in the first part (protocol 1) shows that there were no significant changes in renal hemodynamics, glomerular functions and renal tubular transport in either control group for 120 min or after induced by WEB 2086 over the 90-min perfusion. These results are in agreement with a previous study in the rat IPK, where WEB 2086 also

caused no affect (Monteiro et al., 1999).

The effect of exogenous PAF administration at either a low (95 nM) or a high (270 nM) dose in the rabbit IPK increased both the PP and RVR throughout the 90-min perfusion time compared to the control. These results demonstrate that exogenous PAF induced renal vasoconstriction in the rabbit IPK, which appears contradictory to previous *in vitro* studies in rats and hamsters that showed that PAF dilates some vascular beds and constricts others (Kamata et al., 1989; Dillon et al., 1988). However, some studies have shown a sustained renal vasodilation after the injection of PAF in the rat IPK model (Schwertschlag et al., 1987). The reason for this discrepancy is not clear, although the rat IPK has become
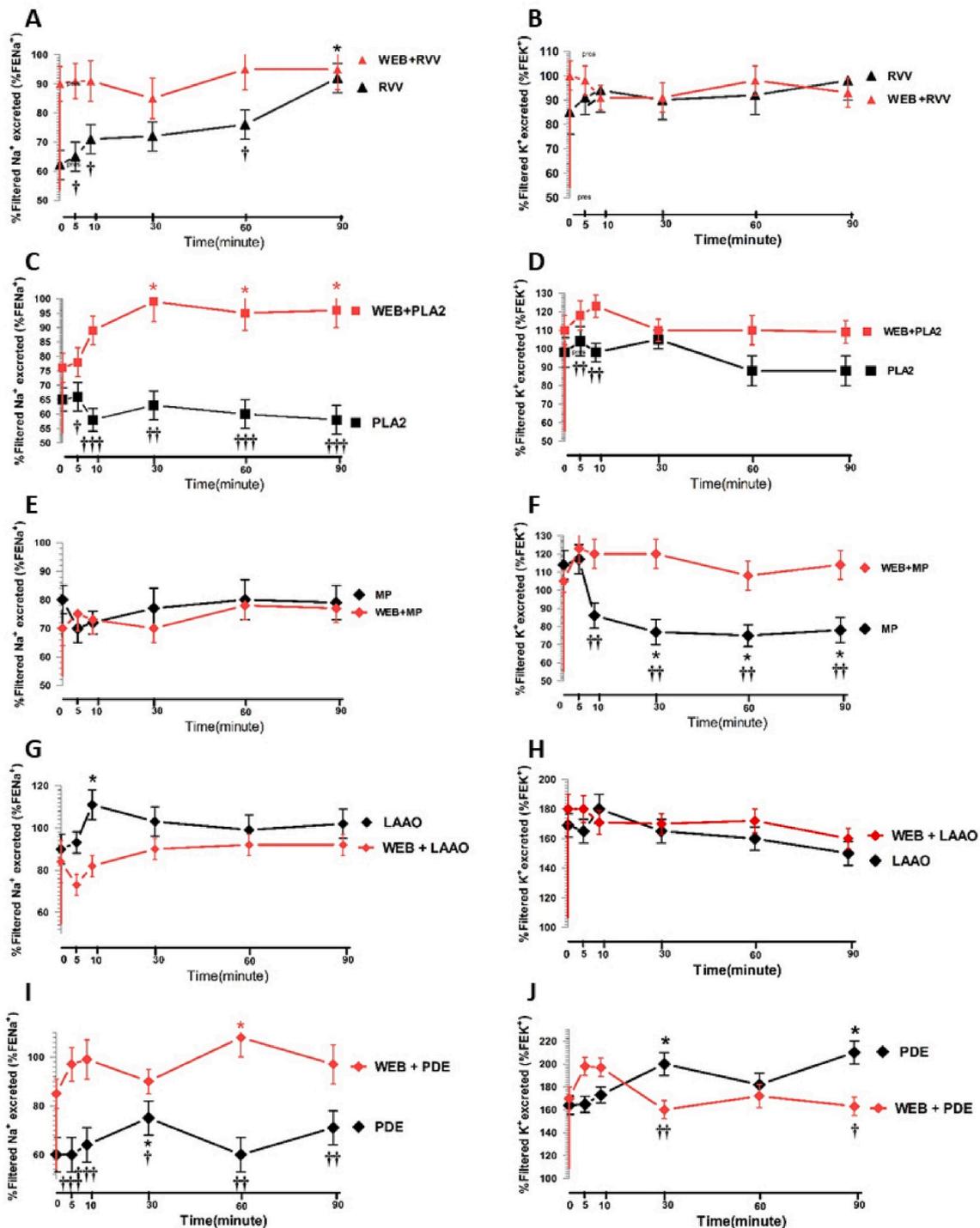
Fig. 8. Changes in the mean %FENa$^+$ and %FEK$^+$ in response to RVV or its fractions with or without WEB 2086 pretreatment in the rabbit IPK. Comparison between groups treated with or without WEB 2806 pretreatment for RVV(A, B), RvPLA$_2$(C, D), RvMP(E, F), RvLAAO(G, H), and RvPDE(I, J). Data are shown as the mean ± SD of four experimental kidneys. *Significant difference ($P < 0.05$; repeated measures ANOVA with Bonferroni post-hoc test between the specified time point and the internal control in the same group. Comparisons between two sets of data at each specified time point between the treated group without WEB 2086 pretreatment and with WEB 2086 are shown by †$P < 0.05$, ††$P < 0.01$, and †††$P < 0.001$ (unpaired Student's t-test).

recognized as a suitable model for the study of renal functions (Maack, 1980).

In this study, in the same rabbit IPK preparation, pretreatment with WEB 2086 (2 μg/μl) abolished the PAF-L-mediated increase in both the PP and RVR, but only partially abrogated that induced by PAF-H. The PAF concentration in PAF-H was 2.84-fold higher than that in PAF-L and so the partial inhibition of PAF-H by WEB 2086 may reflect an insufficient amount of WEB 2086 to abolish the direct renal vasoconstricting

effects. In addition, a number of studies have previously demonstrated that the concentrations of PAF in the renal circulation lies between 0.5 and 2 nM (Badr et al., 1989; Tolins et al., 1989; Wang and Dunn, 1987), and micropuncture studies on isolated rabbit afferent arterioles demonstrated that the direct action of PAF showed a receptor-mediated biphasic effect by dilating them at low concentrations (0.44 nM) while constricting them at higher concentrations (Juncos et al., 1993).

Therefore, the exogenous PAF administration at either PAF-L (95
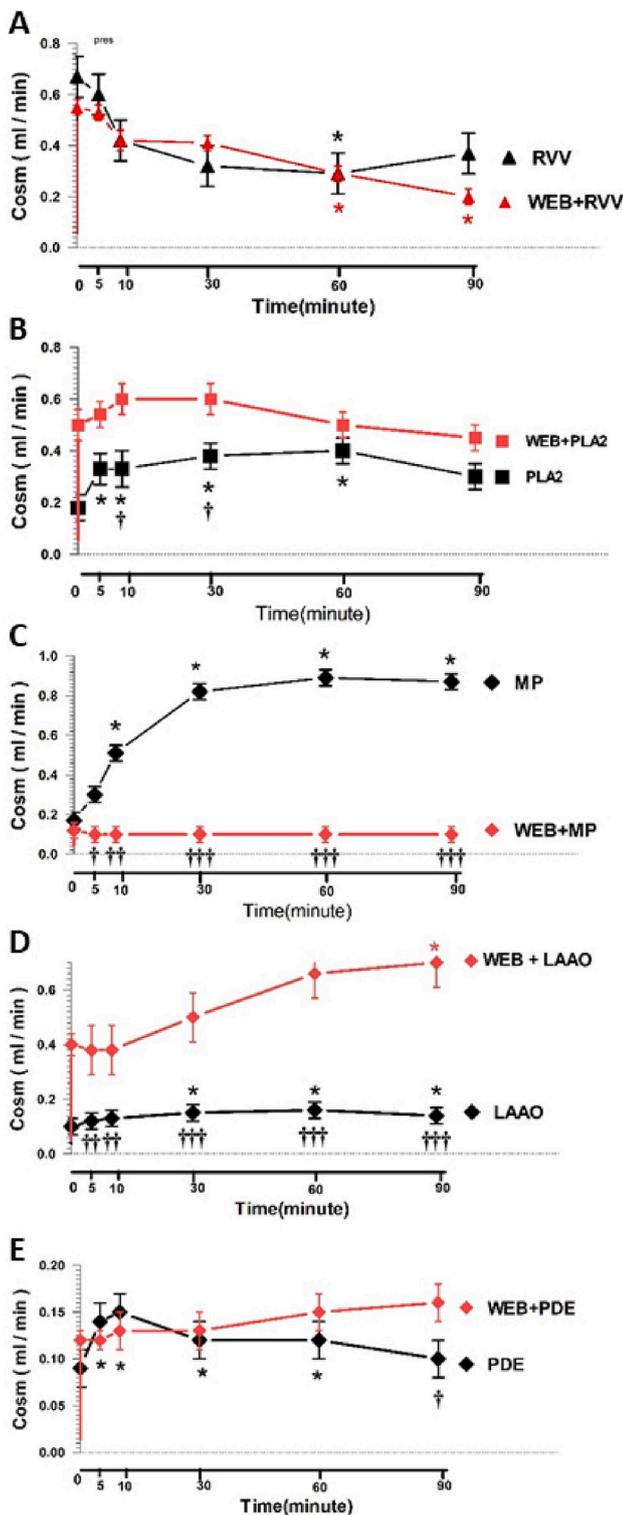
Fig. 9. Changes in the mean Cosm in response to RVV or its fractions with or without WEB 2086 pretreatment in the rabbit IPK. Comparison between groups treated with or without WEB 2806 pretreatment for RVV(A), RvPLA₂(B), RvMP (C), RvLAAO(D), and RvPDE(E). Data are shown as the mean ± SD of four experimental kidneys. *Significant difference ($P < 0.05$; repeated measures ANOVA with Bonferroni post-hoc test between the specified time point and the internal control in the same group. Comparisons between two sets of data at each specified time point between the treated group without WEB 2086 pretreatment and with WEB 2086 are shown by †$P < 0.05$, ††$P < 0.01$, and †††$P < 0.001$ (unpaired Student's t-test).

Table 1

Effects of RVV and its fractions (RvPLA₂, RvMP, RvLAAO, and RvPDE) with or without WEB 2086 pre-treatment on the urinary NO concentration in the rabbit IPK.

Variables: groups	Basal	5 min	10 min	30 min	60 min	90 min
Urinary NO (mM):						
Control	0.75 ± 0.02	0.74 ± 0.04	0.75 ± 0.04	0.78 ± 0.06	0.80 ± 0.10	0.78 ± 0.02
WEB 2086	0.88 ± 0.16	0.77 ± 0.11	0.79 ± 0.10	0.79 ± 0.06	0.83 ± 0.12	0.80 ± 0.08
RVV	1.05 ± 0.06	0.98 ± 0.18	1.03 ± 0.16	0.99 ± 0.10	0.97 ± 0.06	1.08 ± 0.06
WEB 2086 + RVV	0.80 ± 0.08	0.82 ± 0.06	0.84 ± 0.14	0.86 ± 0.12	0.88 ± 0.12	0.88 ± 0.08
RvPLA₂	1.26 ± 0.26	1.13 ± 0.42	1.15 ± 0.18	1.08 ± 0.30	1.20 ± 0.28	1.15 ± 0.24
WEB 2086 + RvPLA₂	0.84 ± 0.26	0.89 ± 0.28	0.88 ± 0.34	0.85 ± 0.28	0.89 ± 0.12	0.91 ± 0.14
RvMP	0.93 ± 0.12	0.85 ± 0.42	0.88 ± 0.16	0.87 ± 0.12	0.90 ± 0.06	0.97 ± 0.16
WEB 2086 + RvMP	0.85 ± 0.08	1.02 ± 0.06	0.90 ± 0.14	0.91 ± 0.18	0.96 ± 0.10	0.87 ± 0.16
RvLAAO	0.95 ± 0.16	0.74 ± 0.18	0.94 ± 0.09	0.86 ± 0.10	0.89 ± 0.24	0.88 ± 0.24
WEB 2086 + RvLAAO	0.91 ± 0.16	0.96 ± 0.16	0.96 ± 0.04	0.87 ± 0.12	0.94 ± 0.18	1.11 ± 0.12
RvPDE	0.98 ± 0.26	0.97 ± 0.24	0.91 ± 0.14	0.94 ± 0.16	0.89 ± 0.12	0.90 ± 0.10
WEB 2086 + RvPDE	0.86 ± 0.18	0.93 ± 0.06	0.86 ± 0.18	0.94 ± 0.14	1.09 ± 0.08	0.82 ± 0.10

Data are presented as the mean ± SD of four perfused kidneys from four different animals in each group. *P*-values analyzed by repeated measures ANOVA with Bonferroni post hoc test: *$P < 0.05$, mean values of specified time period with respect to the basal period in the same group. Basal is the internal control period prior to treatment of each experimental group. WEB 2086 was added 30 min before the specified treatment of each experimental group. Comparison of two sets of data at each specified time point between the treated group alone and the treated group pretreatment with WEB 2086 using unpaired Student's t-test. For calculations, samplings were made at 5, 10, 30, 60, and 90 min after the basal measurements of each experiment. No significant changes in urinary NO concentrations (0.75–1.26 mM) at any point in all treated groups after 90 min of the perfusion time.

nM) or PAF-H (270 nmM) in this study was some 200- to 700-fold higher than those in other reports, which might have contributed to the observed renal vasoconstriction. However, it has been reported that PAF can induce renal vasoconstriction, at least in part, by stimulating production of thromboxane in the IPK model (Camussi, 1986). The greater degree of renal vasoconstriction induced by the exogenous PAF-H administration may then have possibly involved a greater production of thromboxane.

Administration of exogenouse PAF-L caused slight reductions in the GFR, while the UF, including the %FENa, %FEK and Cosm, were progressively increased throughout the perfusion time. In contrast, administration of PAF-H showed elevations of the GFR, UF, %FENa, % FEK, and Cosm. These results suggest that PAF modulates glomerular functions in a complex way that depends on the dosage employed. It has been reported that PAF exerts its effect on a specific PAF receptor within the renal glomeruli (Honda et al., 2002) and increases the glomerular capillary permeability (Pirotzky et al., 1985). The possibility is that PAF-H loading may cause more binding to its specific receptors, activating glomerular capillary permeability and so lead to glomerular cytoskeleton alterations, enhancing the filtrate traffic across the glomerular capillary wall and so resulting in an increased GFR, UF, % FENa, %FEK, and Cosm. However, these effects were prevented by WEB 2086 pretreatment, especially for the low PAF dose (PAF-L).

The second part (protocol 2) of this study involved further evaluation of the pathophysiological mechanisms of the AKI induced by RVV and its fractions. The mechanisms that cause AKI have been suggested (Sitprija
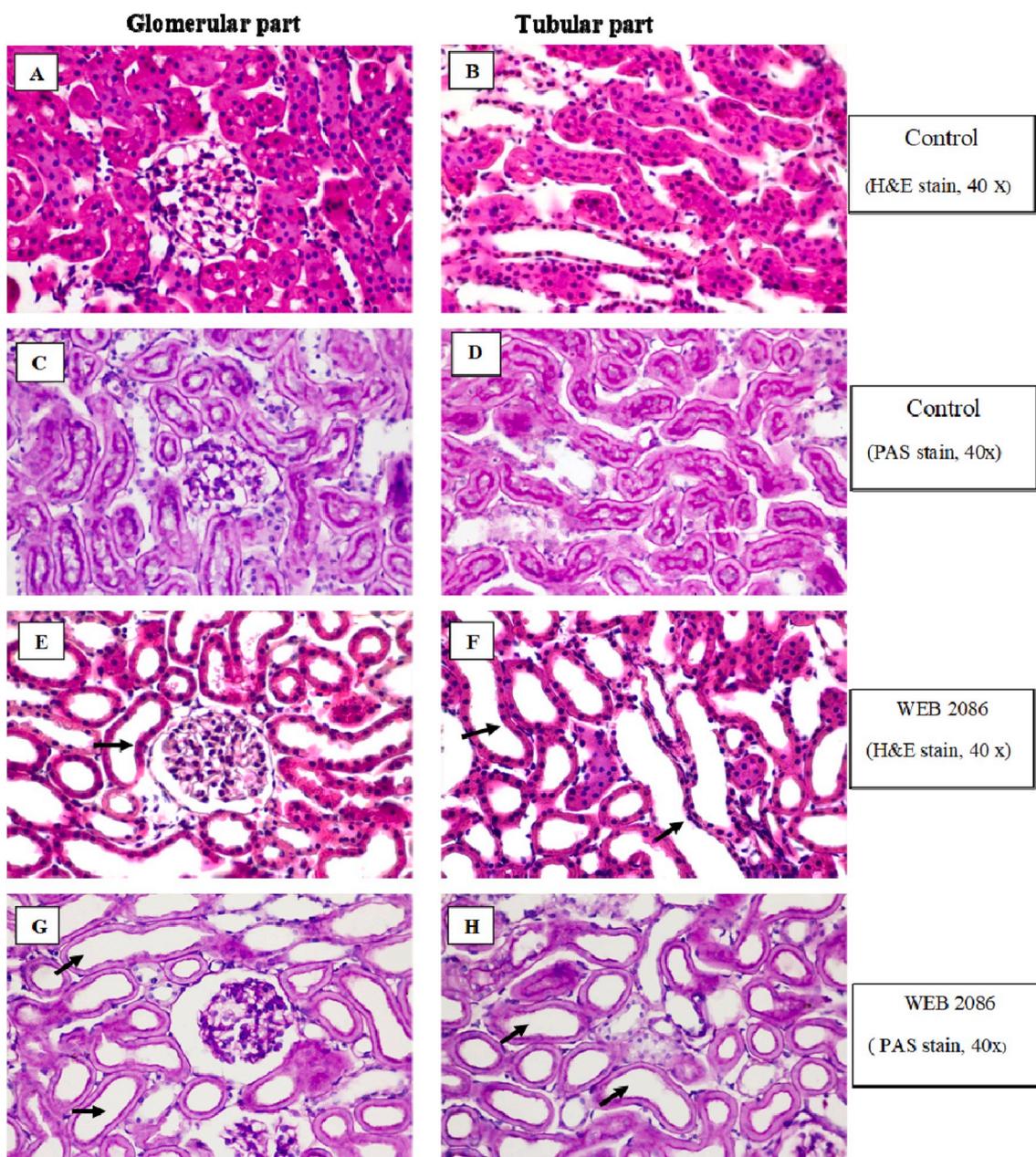
Fig. 10. Representative photomicrographs of kidney sections stained with H&E (A, B, E, F) and PAS (C, D, G, H) of the glomerular and tubular parts of the rabbit IPK (all slides: original magnification 40×). Kidney sections were taken 120 min after perfusion with MKHS alone(A–D) or 90 min after post-administration of WEB 2086 (E–H). Note the morphological normal brush border in the proximal convoluted tubule with PAS staining in both the control and WEB 2086 treated IPK. There was no remarkable lesions in both the glomerular and tubular parts in both the control and WEB 2086 treated IPK, except for a dilated lumen of the proximal and distal convoluted tubules after WEB 2086 treatment (black arrows).

and Chaiyabutr, 1999) which associated with DIC (Swe et al., 1997) or coagulative process in the Viperidae family (Win-Aung et al., 1998). However, DIC has no relevance to the present *in vitro* studies in the rabbit IPK, since the perfusate used in the rabbit IPK lacks fibrinogen and clotting factors.

In the present study, the IPK experimental setup employed RVV at 1 mg/100 ml of perfusate, which was assumed to be equilivant to that of the $2 \times LD_{50}$ of the crude RVV used (0.5 mg/kg BW, i. v.) *in vivo* in experimental dogs (Tungthanathanich et al., 1986) and rabbits (Chaiyabutr et al., 2014). The RVV used in this study in the rabbit IPK produced changes as a temporally biphasic response for both PP and RVR, in agreement with an earlier report (Chaiyabutr et al., 2014). The biphasic response showed an initial transient decrease in the PP followed by a gradual rise in both the PP and RVR over the first 10 min of

perfusion, which indicates that the decrease in PP occurs through the initial renal vasodilation, thereby decreasing the RVR. Similar biphasic responses in the systemic blood pressure by RVV *in vivo* in experimental dogs has been reported (Tungthanathanich et al., 1986), while Chaiyabutr et al. (1984, 1985a) demonstrated that the increase in the systemic blood pressure following the initial transient decrease in RVV-envenomated animals is due to a compensatory mechanism that involves release of vasoconstrictor mediators, either catecholamines or the renin angiotensin system.

It is known that the IPK has a cell-free medium without interference from systemic factors, which is of paramount importance, since it eliminates the involvement of endogenous inflammatory mediators that are not present in this system. However, a number of studies have demonstrated that PAF as an inflammatory mediator can be released by
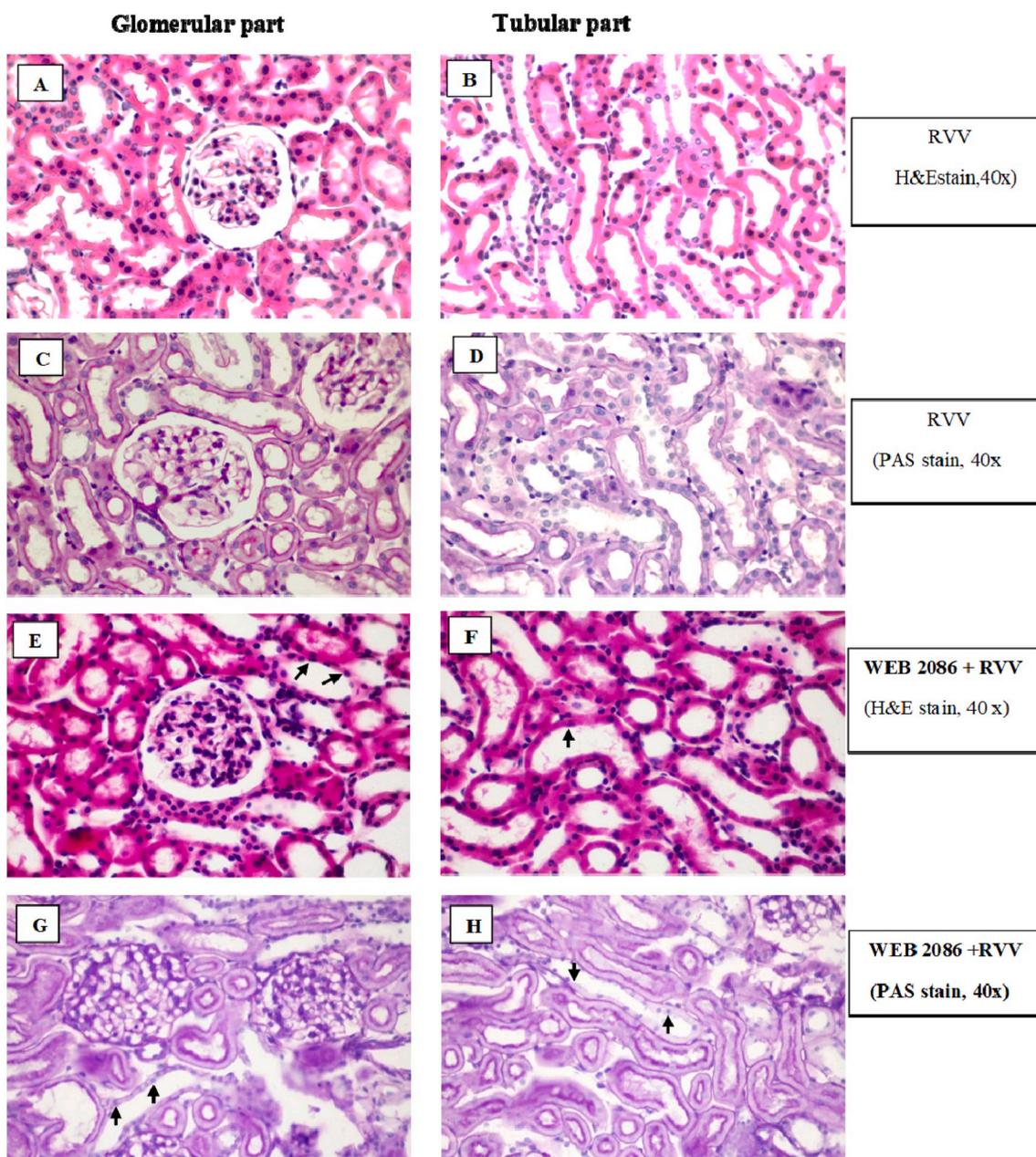
Fig. 11. Representative photomicrographs of kidney sections stained with) H&E (A, B, E, F or PAS (C, D, G, H) of the glomerular and tubular parts of the rabbit IPK (all slides: original magnification 40×). Kidney sections of both the glomerular and tubular parts are from the rabbit IPK 90 min after administration of RVV without (A–D) or with WEB 2086 pretreatment(E–H). Note no distinct brush border was apparent in the proximal convoluted tubules in the IPK treated with RVV without (D) or with WEB2086 pretreatment (H). The IPK treated with RVV showed no remarkable lesion in glomerular parts, while the proximal and distal convoluted tubules revealed dilatation and moderate (+2) tubulonephrosis and the collecting duct had severe (+3) tubulonephrosis (black arrows). The IPK pretreated with WEB before RVV showed no remarkable lesions in the glomerular part, while the proximal and distal convoluted tubules revealed dilatation and mild (+1) tubulonephrosis and the collecting ducts had mild (+1) tubulonephrosis (black arrows).

kidney cells in response to the stimuli of inflammatory cytokines and endotoxins, such as glomerular cells (Morell et al., 1988), endothelial cells (Whatley et al., 1989), and renal mesangial and medullary interstitial cells (Schlondorff and Neuwirth, 1986), including in the IPK (Pirotzky et al., 1984b). However, under basal conditions, no release of the PAF product by resting kidney cells has been noted (Neuwirth et al., 1989). Nevertheless, PAF was shown to be released by kidney tissues during envenoming by *Bothrops jararaca* in the rat IPK, and so was involved as a mediator of the *B. jararaca* venom effects on renal functions (Monteiro and Fonteles, 1999). Thus, we speculated that RVV and its venom fractions may promote the release of PAF synthesized by kidney cells in the rabbit IPK model.

The present study strengthened the findings that PAF is indeed involved as a mediator of the RVV effect on the vasoactive parameters of PP and RVR. The elevation of both PP and RVR was completely abolished by pretreatment with WEB 2086 (2 μg/μl). The changes in the biphasic response in the renal hemodynamics (both PP and RVR) led us to postulate that the liberation of PAF from kidney cells induced by RVV acted as either a vasodilator or a vasoconstrictor, depending upon its concentration (Lo'pez-Novoa, 1999). Then, the released PAF would exert via its receptors the biphasic effects on afferent arterioles, dilating them at low PAF concentrations during the initial period after RVV administration. However, the kidney cells in the rabbit IPK were flooded with perfusate containing RVV in the recirculating system, and so
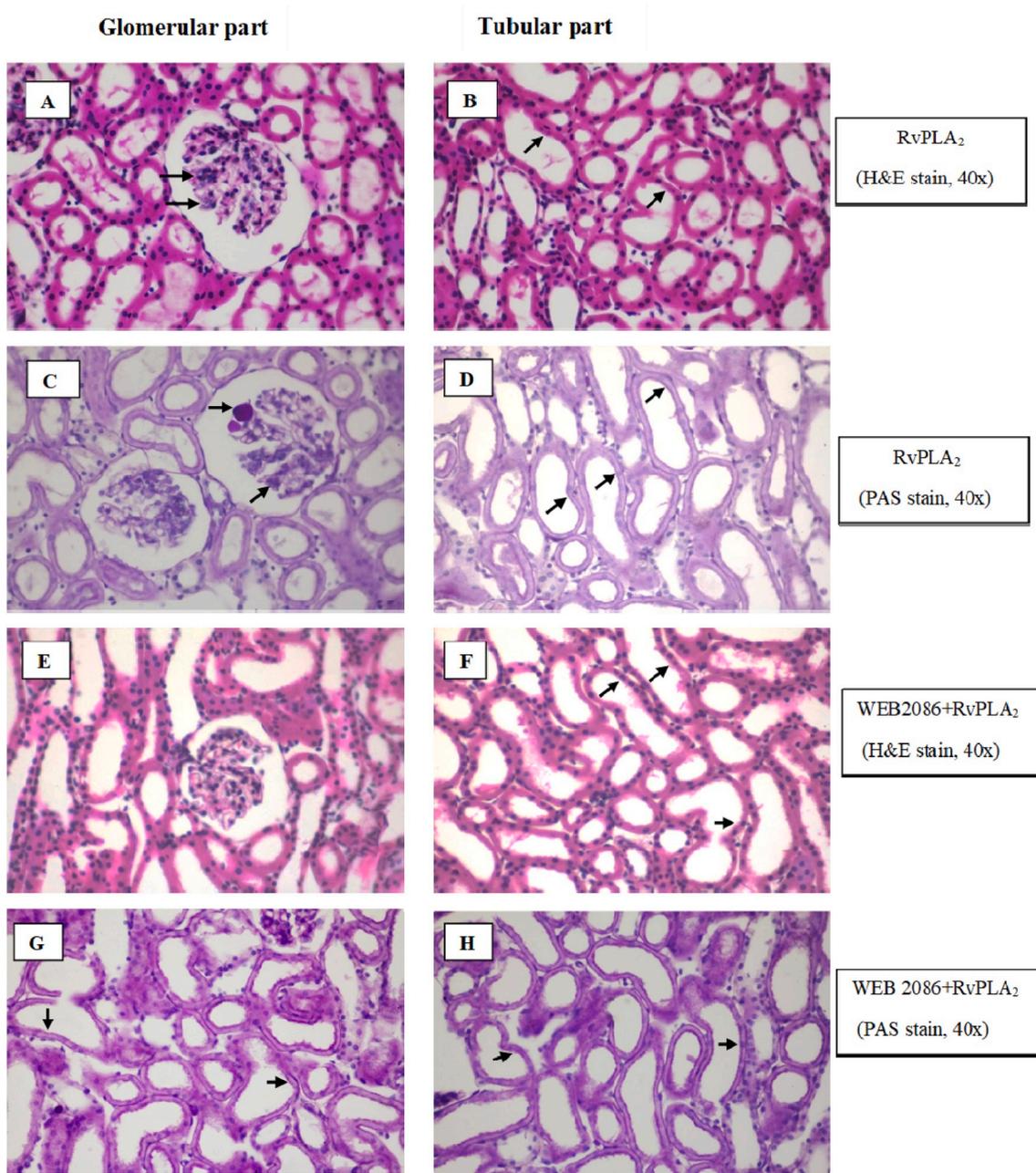
Fig. 12. Representative photomicrographs of rabbit IPK sections stained with H&E (A, B, E, F) and PAS (C, D, G, H) showing the glomerular and tubular parts (all slides: original magnification 40×). Kidney sections were taken 90 min after administration of RvPLA₂ without (A–D) or with (E–H) WEB 2086 pretreatment. Treatment with RvPLA₂ alone resulted in some severe unidentified crystal deposits in the glomerular capillary lumen (A, C; black arrows), while (B, D) the proximal and distal convoluted tubules revealed dilatation and moderate (+3) tubulonephrosis, while the collecting ducts had moderate (+2) tubulonephrosis. Pretreatment with WEB 2086 before PLA₂ showed no remarkable lesions in the glomerular part but the proximal and distal convoluted tubules revealed dilatation and severe (+3) tubulonephrosis and the collecting ducts had severe (+3) tubulonephrosis (black arrows).

became maximally stimulated with a longer exposure time, leading to a further release of PAF products and an accumulation of PAF (increased concentration) within the renal tissue. Therefore, the constricting effect of renal arterioles would be apparent later and last until the end of the remaining 90-min perfusion period.

It is suggested that the locally released PAF into the kidney plays a major role as a mediator and is responsible for the effect of RVV on renal vascular contraction. A direct effect of PAF on contracting afferent arterioles in raising the RVR has been noted (Juncos et al., 1993). However, the mechanism that PAF exerts to obtain the receptor-mediated biphasic effect on afferent arterioles does not relate to other vasoconstrictor mediators, especially the renin-angiotensin system

(Schwertschlag et al., 1987) and sympathetic nervous system (Caillard et al., 1982; Smith et al., 1982), which can interact with the formation of PAF. Since in this present study, there is neither sympathetic innervations to the IPK nor renin substrate in the preparation, an interaction of PAF with these systems would not be likely.

In addition, it has reported that the enhanced NO synthesis might be an important mechanism countering PAF-induced vasoconstriction (Juncos et al., 1993). If so, augmentation of PAF-induced vasoconstriction should be apparent when NO synthesis is decreased or subjected to NO inhibition. However, no significant changes in the urinary NO concentrations was detected at any point in all the treated groups during the 90-min residual perfusion period, indicating that PAF plays a role that is
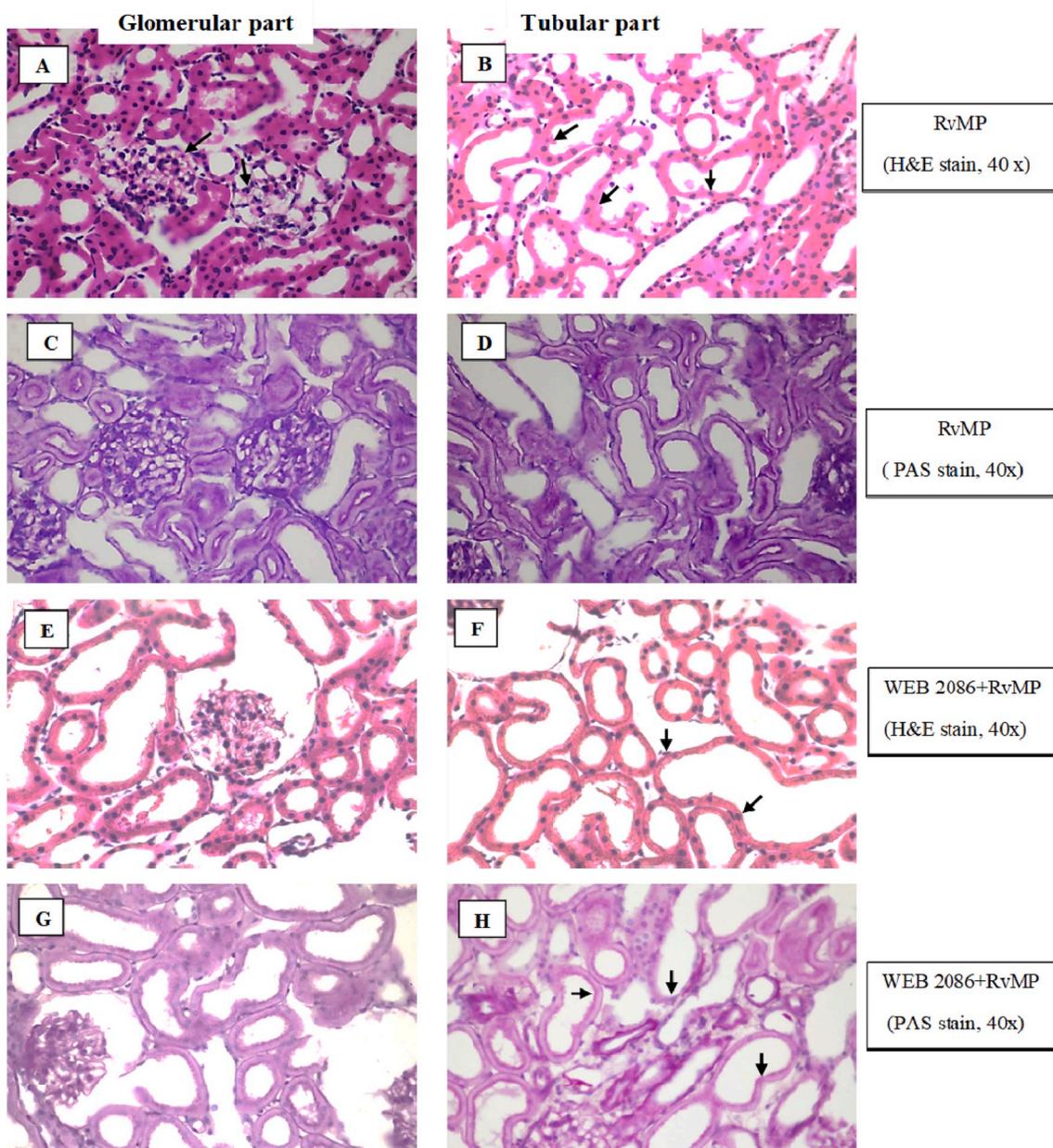
Fig. 13. Representative photomicrographs of rabbit IPK sections stained with H&E(A, B, E, F) and PAS(C, D, G, H) showing the glomerular and tubular parts (all slides: original magnification 40×). Kidney sections were taken 90 min after administration of RvMP without(A–D) or with (E–H) WEB 2086 pretreatment. Treatment with RvMP alone resulted in some severe unidentified crystal deposits in the glomerular capillary lumen (A, C; black arrows), while (B, D) the proximal and distal convoluted tubules revealed dilatation and severe (+3) tubulonephrosis, while the collecting ducts had severe (+3) tubulonephrosis. Pretreatment with WEB 2086 before RvMP showed no remarkable lesions in the glomerular part but the proximal and distal convoluted tubules revealed dilatation and severe (+3) tubulonephrosis and the collecting ducts had severe (+3) tubulonephrosis (F, H; black arrows).

independent of signal transduction pathways for NO production. Thus, a direct role for NO in inhibiting PAF during RVV envenomation in the IPK model can be ruled out.

The pathophysiological changes in the renal functions in the rabbit IPK treated with each venom fraction (RvPLA$_2$, RvMP, RvLAAO, and RvPDE) was examined and compared with that of RVV treatment. It is known that all snake species have different components in their venoms, but PLA$_2$ and MP are the dominant protein families and LAAO and PDE are secondary and minor protein families, respectively, (Tasoulis and Isbister, 2017). The principal component of snake venoms is PLA$_2$ (Bon, 1997), and its pathophysiological effects have been extensively investigated (Kini, 2003). We found that RvPLA$_2$, RvMP, and RvLAAO all caused an increase in the PP and RVR throughout the perfusion period, and for RvPLA$_2$ or RvLAAO, this was not abrogated by WEB 2086

pretreatment. In contrast, the increased PP and RVR mediated by RvMP and RVV were abolished by WEB 2086 pretreatment. This indicates that the action of either RvPLA$_2$ or RvLAAO not only induced the generation of endogenous PAF to cause the renal vasoconstriction, but also involved the disruption of PAF receptor-mediated signaling in renal vasculature.

The increased PP and RVR mediated by RvPLA$_2$ may be explained by both the specific and non-specific actions of PLA$_2$ on the membrane trafficking system. The specific effect of RvPLA$_2$ may involve the pathways of PAF synthesis (Snyder, 1985) and depend on activation of the local calcium concentration (Lo'pez-Novoa, 1999). The specific action of PLA$_2$ is not only directly involved in PAF liberation, but it may also exert its action through digestion of phospholipids in the membranes of vascular smooth muscle cells, leading to cell damage. A major substrate for PAF synthesis is the phospholipid alkyl-acyl glycerophosphocholine,

Glomerular part **Tubular part**
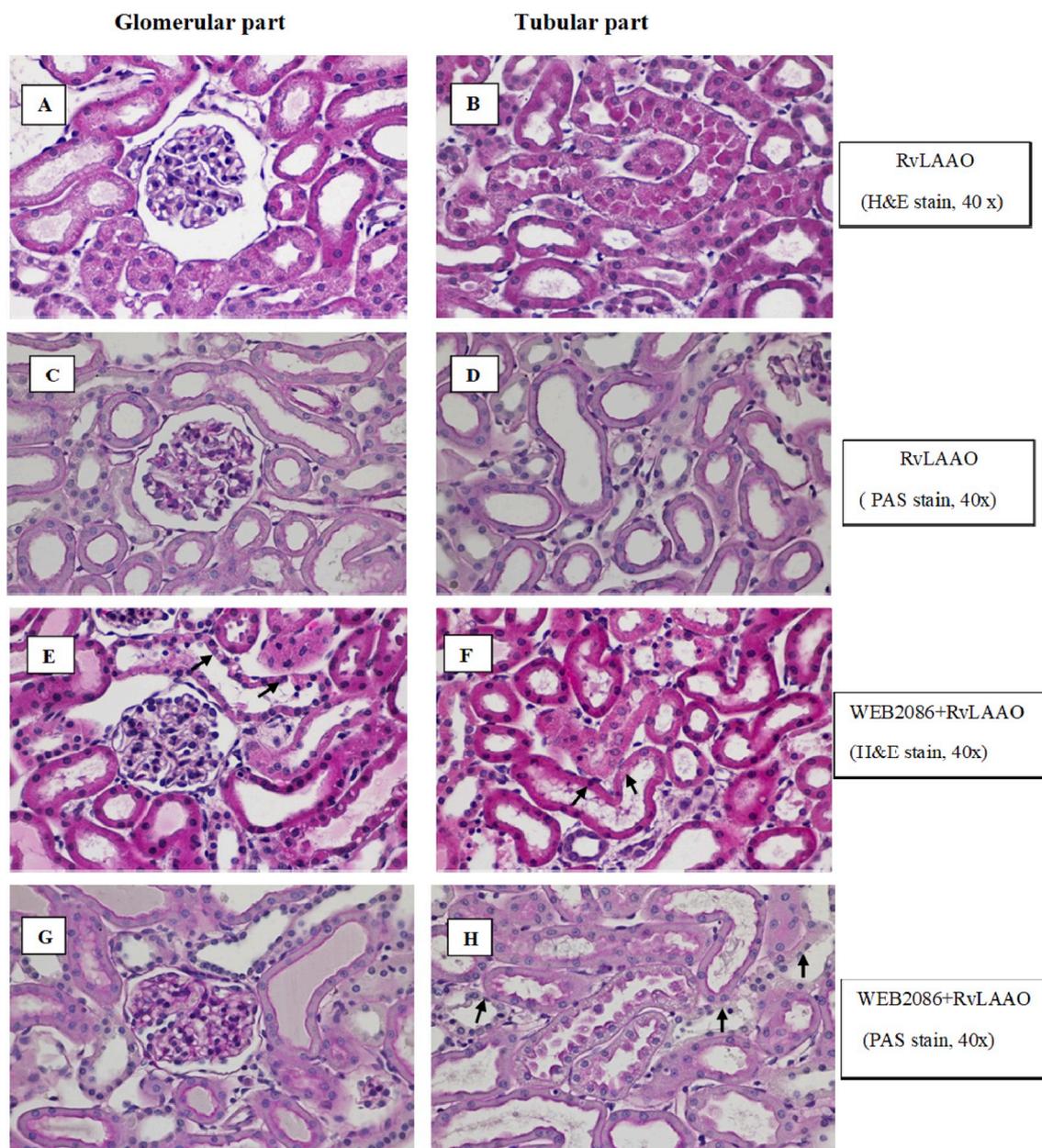
Fig. 14. Representative photomicrographs of rabbit IPK sections stained with H&E (A, B, E, F) and PAS (C, D, G, H) showing the glomerular and tubular parts (all slides: original magnification 40×). Kidney sections were taken 90 min after administration of RvLAAO without (A–D) or with (E–H) WEB 2086 pretreatment. Treatment with RvLAAO alone resulted in severe unidentified crystal deposits in the capillary lumen of some glomerular (A, C), while (B, D) the proximal and distal convoluted tubules revealed dilatation and severe (+3) tubulonephrosis, while the collecting ducts had severe (+3) tubulonephrosis. Pretreatment with WEB 2086 before RvLAAO showed no remarkable lesions in the glomerular part but the proximal and distal convoluted tubules revealed dilatation and severe (+3) tubulonephrosis and the collecting ducts had severe (+3) tubulonephrosis (F, H; black arrows).

which gives rise to lyso-PAF through the action of PLA_2. It was, therefore, speculated that the increased level of PAF may cause contraction of the renal vasculature and/or glomerular mesangial cells. Although an endothelial function was not demonstrated in the present study, previous studies have suggested that increased renal PAF levels coexist with morphological evidence of endothelial damage, in which PAF's vasoconstrictor actions may be stronger (Lo'pez-Novoa, 1999).

Another possible explanation for these results is based on the fact that PLA_2 comprises approximately 20–25% by mass of *Daboia* venom (Sharma et al., 2015; Tan et al., 2018). Thus, the $RvPLA_2$ dose used in this study was approximately 2.6-fold higher than that in the RVV (Fig. 1). This higher specific activity would potentially allow for non-specific toxic effects of $RvPLA_2$ via overt hydrolysis of phospholipids in the cell membranes. However, the IPK model used in this study

is devoid of blood, and so the increases in PP and RVR were not promoted by pro-coagulant events. The $RvPLA_2$ fraction could induce lysis of endothelial cells and so may not only induce the release of PAF but also other vasoconstrictor mediators, which then increase the PP and RVR without abolishment by WEB 2086. Thus, further studies are required to investigate the detailed mechanisms by which PAF activates $RvPLA_2$ activity.

The RvLAAO fraction showed a similar effect to that for $RvPLA_2$, inducing an increase in both the PP and RVR that was not inhibited by WEB 2086 pretreatment. This may be explained by the mechanism of action of LAAO as a homodimeric flavoenzyme that catalyzes the redox reaction of different amino acid groups, generating the catabolic production of hydrogen peroxide (H_2O_2), keto acids, and ammonia (Moustafa et al., 2006; Tan and Fung, 2009). The H_2O_2 generated during

Glomerular part **Tubular part**
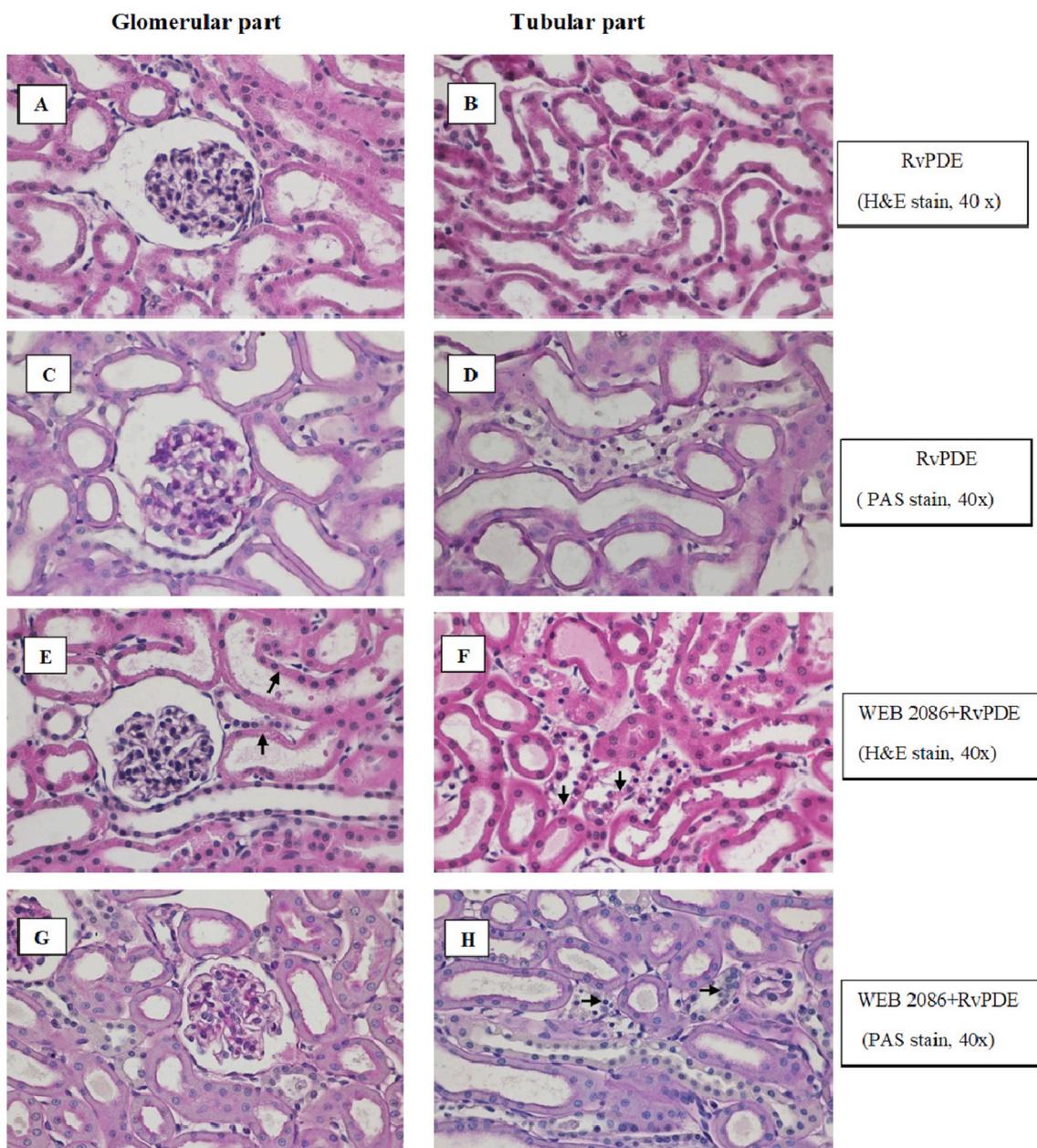
Fig. 15. Representative photomicrographs of rabbit IPK sections stained with H&E (A, B, E, F) and PAS(C, D, G, H) showing the glomerular and tubular parts (all slides: original magnification 40×). Kidney sections were taken 90 min after administration of RvPDE (A–D) without or (E–H) with WEB 2086 pretreatment. Treatment with RvPDE alone resulted in some severe unidentified crystal deposits in the capillary lumen of some glomeruli (A, C), while (B, D) the proximal and distal convoluted tubules revealed dilatation and severe (+3) tubulonephrosis, while the collecting ducts had severe (+3) tubulonephrosis. Pretreatment with WEB 2086 before RvPDE showed no remarkable lesions in the glomerular part but the proximal and distal convoluted tubules revealed dilatation and severe (+3) tubulonephrosis and the collecting ducts had severe (+3) tubulonephrosis (F, H; black arrows).

the enzymatic reaction is a highly toxic reactive oxygen species (ROS) that is capable of acting on intracellular components and cell membranes. The cytotoxicity caused by LAAO through H_2O_2 production triggers autophagy, apoptosis, and necrosis in target cells (Zuliani et al., 2009). This ROS may act directly on cell membranes, leading to an altered permeability of the attacked area and induce endothelial injury (Du and Clemetson, 2002). Thus, it suggests that RvLAAO acts exclusively via a separate mechanism.

The RvLAAO induced lysis of endothelial cells not only releases PAF but also other vasoconstrictor mediators, which could then increase the PP and RVR and so be independent of WEB 2086 inhibition. However, this is not consistent with the findings from another study identifying the role of the LAAO fraction from *Bothrops marajoensis* venom, which

caused significant reductions in the PP and RVR at 90 and 120 min of perfusion time in the rat IPK model (Dantas et al., 2015). The differences in the pathophysiological responses between RvLAAO and the LAAO from *Bothrops* snake may be explained, at least in part, by the different doses of LAAO used in these studies. The LAAO fraction used in the rat IPK (10 µg/ml of perfusate) by Dantas et al. (2015), was about four times higher than the RvLAAO dose used in the present study in the rabbit IPK (2.7 µg/ml of perfusate). Accordingly, the differences in the observed renal hemodynamics to LAAO from these two snake species may not only be due to inherent differences in the LAAO molecules but also to differences in the LAAO level and so expression of the proteolytic activity against amino acids resulting in a higher production of H_2O_2 (Bregge-Silva et al., 2012), causing oxidative stress in the target cell.

In addition, it is speculated that the endothelial injurious stimuli of the RvPLA$_2$ or RvLAAO fractions may cause the localized loss of cellular homeostasis of endothelial cells including cellular energy and membrane permeability to ions transport. Disruption of the plasma membrane integrity may lead to open sodium channels (ENaC) on the vascular smooth muscle cells as it does in epithelial cells (Garcia-Caballero et al., 2011; Jernigan and Drummond, 2005; Rossier and Stutts, 2009). The Na$^+$ influx then causes membrane depolarization and opening of calcium channels, which results in a Ca^{2+} influx. The increased cytosolic Ca^{2+} can cause vascular contraction. Both PP and RVR were, therefore, increased, independent of PAF.

The RvMP fraction also induced a significant increase in the PP and RVR at 60 and 90 min of perfusion time relative to that of RvPLA$_2$, and was also abrogated by WEB 2086 pretreatment. The pattern of changes was similar to that induced by RVV following pretreatment with WEB 2086. This similarity suggests that the RvMP fraction may, at least in part, be responsible for the renal hemodynamic effect of RVV. The RvMP constitutes around 9% by mass of the venom in *Daboia siamensis* venom from China (Tan et al., 2018) and the specific activity of RvMP in the present study was approximately 2.5-fold higher than that of RVV (Fig. 1), implying that the RvMP fraction is a major contributor to the RVV regulation of renal hemodynamics. It is known that the hydrolytic activity of the MPs from snake venoms play multiple roles in the local and systemic effects (Gutiérrez and Rucavado, 2000). Degradation of extracellular matrix (ECM) proteins by MP has been noted (Baramova et al., 1989). It is possible that degradation of the ECM proteins by RvMP could lead to loss of the basement membrane structural and functional integrity, and so affect the kidney cells, especially the vascular smooth muscle, including renal mesangial cells and renal medullary interstitial cells. The generation of PAF in response to the effects induced by the RvMP fraction would occur at those sites (Schlondorff and Neuwirth, 1986). The disruption of the PAF receptor-mediated signaling in the renal vasculature may not be affected by RvMP. Therefore, the enhanced PAF liberation induced by RvMP may mediate the renal vasoconstriction leading to the increased PP and RVR.

In contrast to other venom fractions, RvPDE caused a progressive reduction in both the PP and RVR throughout the perfusion time, and these vasoactive effects were not prevented by WEB 2086 pretreatment, indicating that the reduced renal hemodynamics by RvPDE was not directly mediated by liberation of PAF. Tan et al. (2018) reported that PDE constitutes around 0.25% by mass of the dried venom of *D. siamensis* from Guanxi, China. It is possible that the catabolizing activity of PDE may be inadequate to promote endogenous PAF as a mediator of renal vasoconstriction in this rabbit IPK model. Another explanation for the reduced renal hemodynamics is the hydrolytic activity of PDE associated with cell membranes could catabolize intracellular cAMP or cGMP, which play a role as second messengers in intracellular signaling pathways (Beavo, 1995). The action of PDE has been shown to hydrolyse the 3′-phosphoester bond of cAMP to its biologically inactive 2′, 3′-cAMP-adenosine pathway (3′-AMP and 2′-AMP) and subsequently metabolize to adenosine and inosine (Jackson et al., 2009). If this is the case, one would expect that the catalytic activity of exogenouse RvPDE to decrease the cAMP level in endothelial cells in the rabbit IPK model, which would reduce the protection from hypoxemia induced endothelial injury (Ogawa et al., 1992) leading to vascular relaxation.

We predicted that the RvPDE fraction hydrolyses c-AMP within renal vascular cells to increase adenosine and inosine levels. Since, adenosine is an important regulator of vascular tone, it may also be possible that the increased level of adenosine induced the relaxation of vascular smooth muscle by inhibiting calcium channel activity (Herlihy et al., 1976), leading to vasodilation independent of PAF (Dhananjaya and D'souza, 2010). Actually, different isoforms of PDE have been identified to localize to the glomeruli, mesangial cells, cortical tubules, and inner medullary collecting duct, which plays a role in the regulation of renal hemodynamics and kidney excretory function (Dousa, 1999).

Changes in glomerular functions during envenomation with RVV induced significant progressive reductions in both the GFR and UF independent of PAF (not affected by WEB, 2086 pretreatment). This is the opposite effect to that on the both PP and RVR, suggesting the PAF effect induced by RVV is mediated mostly on the vasoconstriction of renal vasculature, without influencing the renal glomeruli. However, it has been reported that the release of PAF from endothelial and renal mesangial cells occurs from various stimuli (Snyder et al., 1996). *Bothrops jararacussu* venom was reported to cause the release of PAF in the rat IPK model (Havt et al., 2001).

In the present study, the effect of RVV likely had a similar involvement in PAF liberation in the rabbit IPK, where the progressive reduction in GFR and UF may proceed via PAF liberation that then regulates glomerular function by acting directly through a contraction of mesangial cells (Schlondorff et al., 1986) and so decreases the glomerular surface area.

The question to consider is whether whole RVV stimulation might have promoted the release other substances synthesized by renal cells in IPK such as prostaglandins, cytokines, bradykinin, although *in vivo* changes in the release of cytokines and other inflammatory mediators have been reported in patients bitten by Bothrops and Crotalus snakes (Barraviera et al., 1995). It is possible that RVV induces the release of other mediators in renal tissue, especially the production of thromboxane B$_2$ (TxB$_2$), the stable metabolite of thromboxane A$_2$ (TxA$_2$), which may synergistically enhance mesangial cell contraction and thereby sustain the reduced glomerular filtration surface and ultrafiltration coefficient (Kf) (Mene et al., 1989). Our previous study on the histological analysis of rabbit IPK treated with RVV (10 μg/ml of perfusate) also showed no preservation of renal integrity and dilation of glomerular capillary slits (Chaiyabutr et al., 2014). Destruction of the matrix structure in the glomerulus by the direct action of RVV leads to the loss of Kf coinciding with the release of other vasoconstrictor agents, resulting in a decreased GFR and UF, which was not inhibited by WEB 2086 pretreatment. Thus, the glomerular epithelial damage in this model is also an important cause of the renal alterations induced by RVV that could be another mechanism for the significant and sustained reduction of the GFR and UF (Fig. 7A and B).

In contrast to the effect of RVV, the venom fractions RvPLA$_2$, RvMP, RvLAAO, and RvPDE increased the GFR and UF in the rabbit IPK, which suggests different mechanisms of actions were apparent between RVV and its fractions in the regulation of glomerular functions. In addition, Viperid snake venom is rich in hydrolytic enzymes, both PLA$_2$ and MP (Tan et al., 2018). The significant increases in GFR and UF induced by RvPLA$_2$ and RvMP could be explained, in part, by their respective hydrolytic enzyme properties that act on the cell membrane of renal glomeruli leading to an increased permeability of the glomerular filtering membrane and disruption of the glomerular basement membrane. These effects could then lead to an increased inulin clearance in this model and thereby progressive increases in the GFR and UF.

Normally, PAF exerts its effects via a specific PAF receptor within the renal glomeruli (Honda et al., 2002) and PAF has been reported to be one of the mediators of increased glomerular capillary permeability (Pirotzky et al., 1985). The significant increases in both the GFR and UF induced by RvPLA$_2$ or RvMP in this study were abolished by pretreatment with WEB 2086, supporting that endogenous PAF plays a role as a mediator in the RvPLA$_2$ and RvMP effects on renal glomeruli, and partly contributes its effects along with the hydrolytic activity of PLA$_2$ and MP. That WEB 2086 pretreatment prevented the deleterious effects on the glomerular functions promoted by RvPLA$_2$ and RvMP supports the documented effect of PAF receptor antagonists on reducing histopathological lesions in rabbit models of nephrotoxic nephritis (Livio et al., 1986) and in many kidney diseases with a vascular or glomerular etiology (Ortiz et al., 1991; Lo'pez-Novoa, 1999).

In contrast to the effects of RvPLA$_2$ and RvMP, progressive increases in the GFR and UF were induced by RvLAAO and RvPDE, which was not prevented by WEB 2086 pretreatment and so likely does not involve PAF

receptor-mediated signaling in renal glomeruli. However, these results for RvLAAO do not agree with the earlier report of Dantas et al. (2015), who reported the LAAO from *Bothrops marajoensis* venom caused a decrease in the GFR and UF and in the PP and RVR in the rat IPK. These changes in the glomerular function were related to the flavoenzymes activity of snake venom LAAO, which catalyzes stereospecific oxidative deamination to give rise to alpha keto acids, ammonia, and H_2O_2 (Bregge-Silva et al., 2012; Fox, 2013). The production of H_2O_2 may be the prime cause of enhanced glomerular membrane permeability, and so could be responsible for the increased glomerular ultrafiltration. In the present circumstances, RvLAAO caused a marked increase in the UF, which suggests the glomerular filtrate delivered to renal tubules may be a contributing factor by mechanism(s) not related to PAF.

In addition, RvPDE increased the GFR and UF and these remained elevated throughout the 90-min perfusion time, and these effects were not prevented by WEB 2086 pretreatment, suggesting mechanisms other than involving the PAF receptor. Several evidences have suggested a role for increased cAMP levels in several tissues, either by administration of vasopressin, parathormone, and prostaglandins or by infusion of dibutyryl cyclic AMP in micropuncture experiments (Baylis et al., 1976; Ichikawa and Brenner, 1977), in decreasing the glomerular ultrafiltration. Since PDE plays an ancillary role in promoting catabolizing enzymes and hydrolyzes the 3′-phosphoester bond of cAMP and cGMP (Dhananjaya and D'souza, 2010), it is possible that the hydrolytic activity of RvPDE might cause a reduction in the cAMP/cGMP levels in renal glomeruli, leading to the increased glomerular ultrafiltration independent of PAF in renal glomeruli.

The studies on renal tubular functions revealed that RVV increased the %FENa$^+$ with a significant effect at 90 min of perfusion time, while the %FEK$^+$ showed a tendency to increase but this was not statistically significant. This is consistent with a previous study in the rat IPK model (Ratcliffe et al., 1989). Although RVV increased the %FENa$^+$ and %FEK$^+$, it showed the opposite effect on the GFR and UF, suggesting a different mechanism in the regulation of urinary electrolytes excretion. A previous study demonstrated that the direct effect of RVV was to decrease the absolute tubular Na$^+$ reabsorption in both the proximal tubule and distal nephron in rabbit IPK when using lithium as a marker (Chaiyabutr et al., 2014). Micropuncture studies to measure the transmembrane potential in the proximal tubule of a Triturus kidney revealed that RVV caused depolarization in a dose-dependent manner (Chaiyabutr et al., 1985b), which might involve to the inhibition of Na$^+$-K$^+$-ATPase activity in the renal tubules of both the renal cortex and medulla (Buranakarl et al., 1997).

These findings may provide a mechanistic insight into the cellular events in modulation of ion channels activities (Sitprija and Sitprija, 2012), where RVV inhibits Na$^+$ channel activity by inactivation of Na$^+$-H$^+$ exchange (NHE3) in proximal tubules and Na$^+$ channels (ENaC) in the distal nephron. Subsequently, the elevated cytosolic Na$^+$ would decrease Na$^+$ reabsorption through down-regulation of NHE3 and ENaC at the apical border of the renal tubules. Alternatively, RVV may directly inhibit NHE3 and ENaC activities. These effects on the %FENa$^+$ and %FEK$^+$ induced by RVV were blocked by pretreatment with WEB 2086 throughout the perfusion time, indicating that there are PAF receptors present on the renal tubular epithelium and that the effect of RVV on the renal tubular transport of Na$^+$ and K$^+$ was mediated via endogenous PAF influencing urinary electrolyte excretion independent of changes in GFR. The RVV in this study had a protein mass of 10–150 kDa, which is similar to the 6–130 kDa range for the Indian RVV (Kalita et al., 2018). The large molecular mass venom proteins presumably could not be filtered but would cause the release of endogenous PAF from other glomerular cells that, once filtered by the kidney glomeruli, could promote the renal tubular effects observed in this study. Thus, it is reasonable to postulate that PAF induced by RVV may only act locally on a specific PAF receptor in the glomerular and renal medullary interstitial cells (Asano et al., 1996), but also gain access to the renal tubules through glomerular filtration, although the renal tubules do not produce

PAF directly (Pirotzky et al., 1984b). The mechanism of RVV's action on urinary electrolyte excretion is probably mediated via PAF's regulation of ion channels, where it has been observed to inhibit the membrane Na–K-ATPase in a number of cell types (Catalan et al., 1994; Itadani et al., 1998). Also PAF inhibits solute reabsorption in the medullary thick ascending limb (mTAL) and collecting ducts via a cGMP-dependent pathway (Bailly et al., 1992).

The present data clearly demonstrate that WEB 2086 was able to prevent the RVV effect on the renal tubular Na$^+$ and K$^+$ transport, which were mediated in part by the inhibition of the membrane Na–K-ATPase activity by PAF. As described previously in this report, inhibition of membrane Na–K-ATPase activity by PAF can interfere with the intracellular signaling cascade of ion channels in the down-regulation of NHE3 and ENaC at the apical border of renal tubules. This is emphasized by the blockade caused by WEB 2086. However, the protein mass of RVV (10–150 kDa) may limit its filtration to deliver it to the tubular fluid. The relatively high concentration of RVV, at least in the proximal part of the nephron, may have occurred by secretory mechanisms in the tubular fluid via the peritubular capillary. Further investigation is required to demonstrate its pathophysiological significance of the cellular events in modulation of ion channels activities during envenomation.

Additional information on the direct acute effect of RVV on renal cells was obtained by optical microscopy, which revealed no distinct brush border in the proximal convoluted tubules, a moderate degree of acute dilatation, and severe tubulonephrosis (+3) (Fig. 11D, H). These histological alterations of renal cells induced by RVV are similar to those reported previously (Chaiyabutr et al., 2014). The present data clearly demonstrated that pretreatment with WEB 2086 was able to prevent the deleterious effects promoted by RVV on the %FENa$^+$ and %FEK$^+$. It is possible that the histological alterations affected by RVV may be reduced by WEB 2086, since the role of PAF in nephrotoxic nephritis has been reported, where PAF antagonists could reduce the proteinuria and decrease the histopathological lesions (Livio et al., 1986).

Comparative studies on the pathophysiological alterations of renal tubular function induced by RVV fractions are lacking. In the present study, administration of RvMP decreased the %FENa$^+$ and %FEK$^+$ throughout the perfusion time, but showed a different pattern of changes compared to those effects induced by RvPLA$_2$, RvLAAO, and RvPDE. The marked increase in the GFR by RvMP would account for the decreased %FENa$^+$ and %FEK$^+$. Moreover, RvMP showed the opposite effect of a marked increase in the UF and Cosm (Fig. 7E and F and Fig. 9C) and so these findings may provide a mechanistic insight into the altered renal tubular transport of ions that underlies the regulation of urinary electrolyte excretion by RvMP.

The hydrolytic property of either RvMP or RvPLA$_2$ may be involved in a direct action on renal glomeruli and tubular cells leading to an increased cell membrane permeability and resulting in the localized loss of ion homeostasis. Because of the marked increase in the GFR by RvMP, an increased amount of filtrate would be delivered to the tubular segment. Virtually all the Na$^+$ delivered out of the proximal nephon would be reabsorbed. It has been reported that the MP activity in renal tubular cells caused more degradation of the plasma membrane and the cellular matrix proteins leading to a loss of the basement membrane structural integrity, and so the function of the kidney cells (Baramova et al., 1989).

The optical microscopy demonstrated the direct acute effect of RvMP on renal cells, with evident dilatation and severe tubulonephrosis of both the proximal and distal convoluted tubules, including the collecting ducts (Fig. 13B, D, F, H). Thus, changes in the basement membrane structural integrity probably caused leaky tight junctions that connect neighboring tubular cells and allowed both Na$^+$ and K$^+$ to pass directly between the tubular and extracellular fluids down their concentration gradients, and so decrease the net urinary %FENa$^+$ and %FEK$^+$. Therefore, the permeability of the basal or apical membranes, or both, appears to differ considerably between RvPLA$_2$ and RvMP activity.

The RvMP action on electrolyte transport can be explained by the

paracellular pathway. It is known that transcellular Na$^+$ and K$^+$ movements across the renal tubular cells are regulated via the ion channels activities of NHE3 and ENaC at the apical membrane and Na$^+$-K$^+$-ATPase activity at the basolateral membrane (Sitprija and Sitprija, 2012). The question arises as to whether these processes were reduced in the rabbit IPK by the RvPLA$_2$, RvMP, RvLAAO, and RvPDE fractions.

The possibility exists that the effects of RvPLA$_2$ and RvLAAO mainly adopted transcellular routes for ion movements across the renal tubular epithelium, allowing the increased %FENa$^+$ and decreased %FEK$^+$ (Fig. 8C, D, G, H). Therefore, it was inferred that the basal pump activity can cope with these changes during the RvPLA$_2$ and RvLAAO treatments. However, if the permeability of the tubular membrane is greater in the RvMP treatment, then an increased rate of movement of both Na$^+$ and K$^+$ will pass directly between the tubular and extracellular fluids down their concentration gradients, and this might be greater than the transcellular active Na$^+$ and K$^+$transport. Thus, the effect of RvMP on ion transport can be interpreted by paracellular movements when changes in the reductions of both renal %FENa$^+$ and %FEK$^+$occur under these conditions. The changes in the basement membrane structural integrity induced by RvPLA$_2$ and RvMP was probably the cause of the leaky tight junctions from which Na$^+$ escape into the urine might occur. This would create an osmotic diuretic effect, resulting in an increased Cosm and so an increased UF.

Reductions in both the tubular %FENa$^+$ and %FEK$^+$by RvMP was prevented by WEB 2086 pretreatment, indicating that PAF played a role as a mediator of RvMP-induced changes in the renal tubular Na$^+$ and K$^+$ transport in the rabbit IPK. Although, the kidney tubules do not produce PAF directly, a precursor acetyl-transferase activity has been identified in the glomeruli and in other kidney cells (Pirotzky et al., 1984a). The RvPLA$_2$ and RvMP fractions were approximately 13 kDa and 90 kDa, respectively, (Fig. 1), and so are not filtered but could cause the release of PAF from other glomerulular cells that, once filtered by the glomeruli, would promote the tubular effects observed in this study.

The present studies were extended to demonstrate the tubular excretion of Na$^+$ and K$^+$ during treatment with the RvLAAO or RvPDE fractions. Treatment of RvLAAO showed a slightly increased %FENa$^+$, while the %FEK$^+$ showed a tendency to decline throughout the perfusion time, and these were not inhibited by WEB 2086 pretreatment. Thus, PAF was not directly involved in the renal tubular excretion of Na$^+$ and K$^+$. These results differ from the LAAO from *Bothrops marajoensis* venom, which caused both Na$^+$ and K$^+$ tubular transport in isolated rat kidneys (Dantas et al., 2015). Thus, LAAO from different snake venoms may cause different renal alterations. The flavoenzymes in LAAO catalyze the stereospecific oxidative deamination of L-amino acids to give rise to alpha keto acids, ammonia, and H$_2$O$_2$ (Fox, 2013; Bregge-Silva et al., 2012) may be a contributing factor that enhances the membrane permeability of renal tubular cells and so could be responsible for part of the observed changes in the tubular Na+and K$^+$ transport, but by mechanism(s) that are not related to PAF.

In addition, the RvPDE caused an increased %FENa$^+$, %FEK$^+$ and Cosm with a sustained elevation throughout the 90-min perfusion time, and these effects were prevented by WEB 2086 pretreatment, although a progressive increase in the %FENa$^+$ was still apparent. Thus, the RvPDE-induced generation of PAF is a mediator of the changes in the renal tubular transport of electrolytes, presumably as a result of inhibition of proximal tubular reabsorption. Although, PDE plays a role in promoting catabolizing enzymes and hydrolyzes the 3′-phosphoester bond of cAMP and cGMP (Dhananjaya and D'souza, 2010). Several studies have shown that cAMP and cGMP might play a role in the regulation of electrolyte transport in renal tubular cells. In micropuncture studies (Agus et al., 1971) and rat IPKs (Monteiro et al., 1999), infusion of dibutyryl cAMP directly caused a significant decrease in sodium transport at the proximal segment of the nephron. Thus, the hydrolytic property of RvPDE presumably caused a reduction in the cAMP/cGMP level in renal tubular cells leading to an increased in the tubular %FENa$^+$. The RvPDE effect on the %FENa$^+$ was not impressive compared to the changes in the %

FEK$^+$ and Cosm, which were efficiently blocked by WEB 2086, indicating that another pathway besides the G protein-coupled mechanism is also active in kidney tissues. However, evidence of an interaction between the role of RvPDE on PAF and cAMP/cGMP in the control of ion transport across the tubular cell membrane is required.

Previous studies have shown that the kidney is a major site of arachidonic acid release and its subsequent enzymatic conversion to multiple bioactive prostanoids via the cyclooxygenase metabolic pathway. One such substance that plays an important role in renal physiology is PGE2. Besides exerting its effects on a specific PAF receptor within renal glomeruli (Honda et al., 2002), PAF dose-dependently stimulates the release of PGE2 on rabbit IPKs (Weisman et al., 1985, 1988). The different actions of PGE2 are mediated via different specific G protein-coupled cell surface receptors (Breyer et al., 1996). Multiple effects of PGE2 on the vascular smooth muscle tonus, glomerular filtration, and renal ion and water transport have been described in the rabbit IPK (Yoshida et al., 1986; Hébert et al., 1993, 1995). Direct injection of RVV into the renal artery in dogs increased the renal blood flow and GFR, which was mediated through prostaglandin and reversed by indomethacin (Thamaree et al., 1994). Therefore, future studies may clarify the possible participation of PGE2 in the effects induced by RVV and its fractions that are abolished by WEB 2086 in this pharmacological preparation.

5. Conclusion

The mechanisms by which RVV and its fractions (RvPLA$_2$, RvMP, RvLAAO, and RvPDE) induced renal alterations that cause AKI to develop to ARF, are somehow related to a concomitant generation of PAF. Based on the fact that each venom fraction did not appear to act in a similar manner in terms of the induced changes in the renal functions, they are unlikely to account for that seen by RVV. RVV and most of its fractions increased renal hemodynamics (i.e. PP and RVR) except RvPDE, by which these changes were induced by PAF-dependent (RVV and RvMP) and independent (RvPLA$_2$ RvLAAO and RvPDE) pathways. Meanwhile, RVV caused significant decrease in GFR and UF, while its fractions caused opposite effects, which increased GFR and UF were prevented by WEB2086 for RvPLA$_2$ and RvMP but not for RvLAAO and RvPDE including RVV. In addition, RVV caused an increased %FENa$^+$ and %FEK$^+$ via the renal tubules, which was abrogated by WEB 2086 pretreatment. The increased tubular Na$^+$ and K$^+$ transport induced by RvPLA$_2$, RvLAAO, and RvPDE would be due to their direct action on the tubular membrane, not by PAF pathway since WEB2086 was not able to block the renal tubular effects. The effect of RvMP on tubular sodium transport is probably not influenced by PAF since WEB2086 was also not able to block the action. On the contrary, the effect of RvMP on tubular potassium transport was markedly reduced by the action of PAF since WEB2086 was able to block this effect. The present results, therefore, support the hypothesis that RVV contains several different components that could act either individually or synergistically.

Author contributions

Contributed to the conception and designed the study: NC, LC, TV, PL, OK, AR.

Performed venom fractionations and determined the specific activity: OK, LC, TV, PL.

Contributed reagents/materials/analysis tools: NC, LC, OK, AR.

Performed the animal experiments: NC, LC, TV, PL.

Prepared the histological slices and stainings the kiney tissue: NC, TV, PL, AR.

Evaluated the histological slices: AR, NC.

Analyzed the data and performed the statistics: NC, LC, TV, PL.

Wrote and revised the paper: NC, LC, VS.

All authors contributed to the final version of the manuscript and read and approved the submit version.

Ethical statement

All animal experiments were performed under the procedures and with the approval of the QSMI project number QSMI-ACUC-03-2016 (Pathophysiological actions of Russell's viper venom: The role and mechanism of its fractional components induced acute renal failure. Male adult white New Zealand rabbits used in all experiments were obtained from the laboratory animal facility of QSMI. Animal facility staff as well as research staff were trained in the correct and humane handling of rabbits before the start of any procedure.

Declaration of competing interest

The authors declare that they have no known competing financial interests or personal relationships that could have appeared to influence the work reported in this paper.

Acknowledgements

References

Agus, Z.S., Puschett, J.B., Senesky, D., Goldberg, M., 1971. Mode of action of parathyroid hormone and cyclic adenosine 3', 5'-monophosphate on renal tubular phosphate reabsorption in the dog. J. Clin. Invest. 50, 617–626. https://doi.org/10.1172/JCI106532.

Anson, M.L., 1938. The estimation of pepsin, trypsin, papain, and cathepsin with hemoglobin. J. Gen. Physiol. 22, 79–89. https://doi.org/10.1085/jgp.22.1.79.

Asano, K., Taniguchi, S., Nakao, A., Watanabe, T., Kurokawa, K., 1996. Distribution of platelet activating factor receptor mRNA along the rat nephron segments. Biochem. Biophys. Res. Commun. 225, 352–357. https://doi.org/10.1006/bbrc.1996.1179.

Badr, K.F., DeBoer, D.K., Takahashi, K., Harris, R.C., Fogo, A., Jacobson, H.R., 1989. Glomerular responses to platelet-activating factor in the rat: role of thromboxane A₂. Am. J. Physiol. 256, F35–F43. https://doi.org/10.1152/ajprenal.1989.256.1.F35.

Bailly, C., Barlet-Bas, C., Amiel, C., 1992. Platelet activating factor inhibits Cl and K transport in the medullary thick ascending limb. Kidney Int. 41, 269–274. https://doi.org/10.1038/ki.1992.38.

Baramova, E.N., Shannon, J.D., Bjarnason, J.B., Fox, J.W., 1989. Degradation of extracellular matrix proteins by hemorrhagic metalloproteinases. Arch. Biochem. Biophys. 275, 63–71. https://doi.org/10.1016/0003-9861(89)90350-0.

Barraviera, B., Lomonte, B., Tarkowski, A., Hanson, L.A., Meira, D.A., 1995. Acute phase reactions, including cytokines, in patients bitten by *Bothrops* and *Crotalus* snakes in Brazil. J. Venom. Anim. Toxins 1, 11–22. https://doi.org/10.1590/S0104-79301995000100003.

Baylis, C., Deen, W.M., Myers, B.D., Brenner, B.M., 1976. Effects of some vasodilator drugs on transcapillary fluid exchange in renal cortex. Am. J. Physiol. 230, 1148–1158. https://doi.org/10.1152/ajplegacy.1976.230.4.1148.

Beavo, J.A., 1995. Cyclic nucleotide phosphodiesterases: functional implications of multiple isoforms. Physiol. Rev. 75, 725–748. https://doi.org/10.1152/physrev.1995.75.4.725.

Benveniste, J., Henson, P.M., Cochrane, C.G., 1972. Leucocyte-dependent histamine release from rabbit platelets. The role of IgE, basophils and a platelet-activating factor. J. Exp. Med. 136, 1356–1377. https://doi.org/10.1084/jem.136.6.1356.

Bon, C., 1997. Snake venom and pharmacopoeia. In: Bauchot, R. (Ed.), Snake Natural History, first ed. Sterling Publishing Co., New York, pp. 194–200.

Bregge-Silva, C., Nonato, M.C., de Albuquerque, S., Ho, P.L., Junqueira de Azevedo, I.L. M., Diniz, M.R.V., Lomonte, B., Rucavado, A., Díaz, C., Gutiérrez, J.M., Arantes, E.C., 2012. Isolation and biochemical, functional and structural characterization of a novel L-amino acid oxidase from *Lachesis muta* snake venom. Toxicon 60, 1263–1276. https://doi.org/10.1016/j.toxicon.2012.08.008.

Breyer, M.D., Jacobson, H.R., Breyer, R.M., 1996. Functional and molecular aspects of renal prostaglandin receptors. J. Am. Soc. Nephrol. 7, 8–17. PMID: 8808104.

Buranakarl, C., Kalandakanon, S., Komolvanich, S., Chaiyabutr, N., 1997. Inhibition of the renal Na, K-ATPase by Russell's viper venom. Thai J. Physiol. Sci. 10, 27–36. http://www.j-pbs.org/pdf/101/10_27Buranakarl.pdf.

Caillard, C.G., Mondot, S., Zundel, J.L., Julou, L., 1982. Hypotensive activity of PAF-acether in rats. Agents Actions 12, 725–730. https://doi.org/10.1007/bf01965093.

Camussi, G., 1986. Potential role of platelet-activating factor in renal pathophysiology. Kidney Int. 29, 469–477. https://doi.org/10.1038/ki.1986.23.

Caramelo, C., Fernandez-Gallardo, S., Marin-Cao, D., Iñarrea, P., Santos, J.C., López-Novoa, J.M., Crespo, M.S., 1984. Presence of platelet activating factor in blood from humans and experimental animals. Its absence in anephric individuals. Biochem. Biophys. Res. Commun. 120, 789–796. https://doi.org/10.1016/S0006-291X(84)80176-X.

Casals-Stenzel, J., Heuer, H.O., 1990. Use of WEB 2086 and WEB 2170 as platelet-activating factor antagonists. In: Murphy, R.C., Fitzpatrick, F.A. (Eds.), Methods in

Enzymology, vol. 187. Academic Press, San Diego, California, pp. 455–465. https://doi.org/10.1016/0076-6879(90)87052-5.

Catalan, R.E., Martinez, A.M., Aragones, M.D., Fernandez, I., Miguel, B.G., Calcerrada, M.C., Perez, M.J., 1994. Platelet-activating factor inhibits (Na+, K+) ATPase activity in rat brain. Neurosci. Res. 19, 241–244. https://doi.org/10.1016/0168-0102(94)90149-x.

Chaiyabutr, N., Vasaruchapong, T., Chanhome, L., Rungsipipat, A., Sitprija, V., 2014. Acute effect of Russell's viper (*Daboia siamensis*) venom on renal tubular handling of sodium in isolated rabbit kidney. Asian Biomed. 8, 195–202. https://doi.org/10.5372/1905-7415.0802.279.

Chaiyabutr, N., Sitprija, V., Kato, S., Sugino, N., 1985a. Effects of converting enzyme inhibitor on renal function of rats following Russell's viper venom administration. ICMR (Int. Cent. Med. Res.) Ann. 5, 169–179.

Chaiyabutr, N., Sitprija, V., Sugino, N., Hoshi, T., 1985b. Russell's viper venom-induced depolarization in the proximal tubule of *Triturus* kidney. Thai J. Vet. Med. 15, 297–303.

Chaiyabutr, N., Tungthanathanich, P., Loypetjra, P., Pichaicharnarong, A., Sitprija, V., 1984. Observations on general circulation and renal hemodynamics of experimental dogs given Russell's viper venom. Thai. J. Vet. Med. 14, 256–270.

Dantas, R.T., Jorge, A.R.C., Jorge, R.J.B., de Menezes, R.R.P.P.B., Lima, D.B., Torres, A.F. C., Toyama, M.H., Monteiro, H.S.A., Martins, A.M.C., 2015. L-amino acid oxidase from Bothrops *marajoensis causes* nephrotoxicity in isolated perfused kidney and cytotoxicity in MDCK renal cells. Toxicon 104, 52–56. https://doi.org/10.1016/j.toxicon.2015.08.007.

Dhananjaya, B.L., D'souza, C.J.M., 2010. An overview on nucleases (DNase, RNase, and phosphodiesterase) in snake venoms. Biochem. (Moscow) 75, 1–6. https://doi.org/10.1134/S0006297910010013.

Dillon, P.K., Ritter, A.B., Duran, W.N., 1988. Vasoconstrictor effects of platelet-activating factor in the hamster cheek pouch microcirculation: dose related relations and pathways of action. Circ. Res. 62, 722–731. https://doi.org/10.1161/01.res.62.4.722.

Dousa, T.P., 1999. Cyclic-3',5'-nucleotide phosphodiesterase isozymes in cell biology and pathophysiology of the kidney. Kidney Int. 55, 29–62. https://doi.org/10.1046/j.1523-1755.1999.00233.x.

Du, X.Y., Clemetson, K.J., 2002. Snake venom L-amino acid oxidases. Toxicon 40, 659–665. https://doi.org/10.1016/s0041-0101(02)00102-2.

Fox, J.W., 2013. A brief review of the scientific history of several lesser-known snake venom proteins: L-amino acid oxidases, hyaluronidases and phosphodiesterases. Toxicon 62, 75–82. https://doi.org/10.1016/j.toxicon.2012.09.009.

Garcia-Caballero, A., Ishmael, S.S., Dang, Y., Gillie, D., Bond, J.S., Milgram, S.L., Stutts, M.J., 2011. Activation of the epithelial sodium channel by the metalloprotease meprin B subunit. Channel 5, 14–22. https://doi.org/10.4161/chan.5.1.13759.

Gutiérrez, J.M., Rucavado, A., 2000. Snake venom metalloproteinases: their role in the pathogenesis of local tissue damage. Biochimie 82, 841–850. https://doi.org/10.1016/s0300-9084(00)01163-9.

Harvey, A.L., Bradley, K.N., Cochran, S.A., Rowan, E.G., Pratt, J.A., Quillfeldt, J.A., Jerusalinsky, D.A., 1998. What can toxins tell us for drug discovery? Toxicon 36, 1635–1640. https://doi.org/10.1016/s0041-0101(98)00156-1.

Havt, A., Fonteles, M.C., Monteiro, H.S.A., 2001. The renal effects of *Bothrops jararacussu* venom and the role of PLA(2) and PAF blockers. Toxicon 39, 1841–1846. https://doi.org/10.1016/s0041-0101(01)00146-5.

Hébert, R.L., Jacobson, H.R., Fredin, D., Breyer, M.D., 1993. Evidence that separate PGE2 receptors modulate water and sodium transport in rabbit cortical collecting duct. Am. J. Physiol. 265 (5 Pt 2), F643–F650. https://doi.org/10.1152/ajprenal.1993.265.5.F643.

Hébert, R.L., Breyer, R.M., Jacobson, H.R., Breyer, M.D., 1995. Functional and molecular aspects of prostaglandin E receptors in the cortical collecting duct. Can. J. Physiol. Pharmacol. 73 (2), 172–179. https://doi.org/10.1139/y95-026.

Herlihy, J.T., Bockman, E.L., Berne, R.M., Rubio, R., 1976. Adenosine relaxation of isolated vascular smooth muscle. Am. J. Physiol. 230, 1239–1243. https://doi.org/10.1152/ajplegacy.1976.230.5.1239.

Holzer, M., Mackessy, S.P., 1996. An aqueous endpoint assay of snake venom phospholipase A₂. Toxicon 34, 1149–1155. https://doi.org/10.1016/0041-0101(96)00057-8.

Honda, Z.I., Ishii, S., Shimizu, T., 2002. Platelet-activating factor receptor. J. Biochem. 131, 773–779. https://doi.org/10.1093/oxfordjournals.jbchem.a003164.

Ichikawa, I., Brenner, B.M., 1977. Evidence for glomerular actions of ADH and dibutyryl cyclic AMP in the rat. Am. J. Physiol. 233, F102–F117. https://doi.org/10.1152/ajprenal.1977.233.2.F102.

Itadani, K., Morita, K., Kitayama, S., Imai, Y., Yamaki, H., Akagawa, Y., Dohi, T., 1998. Inhibition of Na+, K (+)-ATPase by platelet activating factor in dog submandibular glands. Prostag. Other Lipid Mediat. 55, 377–385. https://doi.org/10.1016/s0090-6980(98)00031-8.

Jackson, E.K., Ren, J., Mi, Z., 2009. Extracellular 2',3'-cAMP is a source of adenosine. J. Biol. Chem. 284, 33097–33106. https://doi.org/10.1074/jbc.M109.053876.

Jernigan, N.L., Drummond, H.A., 2005. Vascular ENaC proteins are required for renal myogenic constriction. Am. J. Physiol. Ren. Physiol. 289, F891–F901.

Juncos, L.A., Ren, Y.L., Arima, S., Ito, S., 1993. Vasodilator and constrictor actions of platelet-activator factor in the isolated microperfused afferent arteriole of the rabbit kidney: role of endothelium- derived relaxing factor/nitric oxide and cyclooxygenase products. J. Clin. Invest. 91, 1374–1379. https://doi.org/10.1172/JCI116339.

Kalita, B., Patra, A., Das, A., Mukherjee, A.K., 2018. Proteomic analysis and immuno-profiling of eastern India Russell's viper (*Daboia russelii*) venom: correlation between RVV composition and clinical manifestations post RV bite. J. Proteome Res. 17, 2819–2833. https://doi.org/10.1021/acs.jproteome.8b00291.

Kanjanabuch, T., Sitprija, V., 2008. Snakebite nephrotoxicity in asia. Semin. Nephrol. 28, 363–372. https://doi.org/10.1016/j.semnephrol.2008.04.005.

Kamata, K., Mori, T., Shigenobu, K., Kasuya, Y., 1989. Endothelium-dependent vasodilator effects of platelet-activating factor on rat resistance vessels. Br. J. Pharmacol. 98, 1360–1364. https://doi.org/10.1111/j.1476-5381.1989.tb12685.x.

Kini, R.M., 2003. Excitement ahead: structure, function and mechanism of snake venom phospholipase A_2 enzymes. Toxicon 42, 827–840. https://doi.org/10.1016/j.toxicon.2003.11.002.

Livio, M., Morigi, M., Zoja, C., Remuzzi, G., Patrono, C., Bertani, T., 1986. Role of platelet activating factor (PAF) in nephrotoxic nephritis (NTN) demonstrated by a PAF receptor antagonist (Abstract). Kidney Int. 29, 282A.

Lo'pez-Novoa, J.M., 1999. Potential role of platelet activating factor in acute renal failure. Kidney Int. 55, 1672–1682. https://doi.org/10.1046/j.1523-1755.1999.00450.x.

Lo, T.B., Chen, Y.H., Lee, C.Y., 1966. Chemical studies of Formosan cobra (*Naja naja atra*) venom (I). Chromatographic separation of crude venom on CM-Sephadex and preliminary characterization of its components. J. Chin. Chem. Soc. Ser. II. 13, 25–37. https://doi.org/10.1002/jccs.196600004.

Maack, T., 1980. Physiological evaluation of the isolated perfused rat kidney. Am. J. Physiol. 238, F7l–F78. https://doi.org/10.1152/ajprenal.1980.238.2.F71.

Mene, P., Simonson, M.S., Dunn, M.J., 1989. Physiology of the mesangial cell. Physiol. Rev. 69, 1347–1424. https://doi.org/10.1152/physrev.1989.69.4.1347.

Mitrmoonpitak, C., Chulasugandha, P., Khow, O., Noiprom, J., Chaiyabutr, N., Sitprija, V., 2013. Effects of phospholipase A_2 and metalloprotease fractions of Russell's viper venom on cytokines and renal hemodynamics in dogs. Toxicon 61, 47–53. https://doi.org/10.1016/j.toxicon.2012.10.017.

Monteiro, H.S.A., Fonteles, M.C., 1999. The effect of *Bothrops jararaca* venom on rat kidney after short-term exposure: preliminary results. Pharmacol. Toxicol. 85, 198–200. https://doi.org/10.1111/j.1600-0773.1999.tb00092.x.

Monteiro, H.S.A., Lima, A.A.M., Fonteles, M.C., 1999. Glomerular effects of cholera toxin in isolated perfused rat kidney: a potential role for platelet activating factor. Pharmacol. Toxicol. 85, 105–110. https://doi.org/10.1111/j.1600-0773.1999.tb00075.x.

Morell, G.P., Pirotzky, E., Erard, D., Desmottes, R.M., Bidault, J., Damais, C., Benveniste, J., 1988. Paf-acether (platelet-activating factor) and interleukin-1-like cytokine production by lipopolysaccharide-stimulated glomeruli. Clin. Immunol. Immunopath. 46, 396–405. https://doi.org/10.1016/0090-1229(88)90058-X.

Moustafa, I.M., Foster, S., Lyubimov, A.Y., Vrielink, A., 2006. Crystal structure of LAAO from *Calloselasma rhodostoma* with an L-phenylalanine substrate: insights into structure and mechanism. J. Mol. Biol. 364, 991–1002. https://doi.org/10.1016/j.jmb.2006.09.032.

Neuwirth, R., Satriano, J.A., DeCandido, S., Clay, K., Schlondorff, D., 1989. Angiotensin II causes formation of platelet activating factor in cultured rat mesangial cells. Circ. Res. 64, 1224–1229. https://doi.org/10.1161/01.res.64.6.1224.

Ogawa, S., Koga, S., Kuwabara, K., Brett, J., Morrow, B., Morris, S.A., Bilezikian, J.P., Silverstein, S.C., Stern, D., 1992. Hypoxia-induced increased permeability of endothelial monolayers occurs through lowering of cellular cAMP levels. Am. J. Physiol. 262, C546–C554. https://doi.org/10.1152/ajpcell.1992.262.3.C546.

Ortiz, A., Gomez-Chiarri, M., Lerma, J.L., Gonzalez, E., Egido, J., 1991. The role of platelet-activating factor (PAF) in experimental glomerular injury. Lipids 26, 1310–1315. https://doi.org/10.1007/bf02536555.

Pirotzky, E., Ninio, E., Bidault, J., Pfister, A., Benveniste, J., 1984a. Biosynthesis of platelet-activating factor VI. Precursor of platelet-activating factor and acetyltransferase activity in isolated rat kidney cells. Lab. Invest. 51, 567–572. https://www.ncbi.nlm.nih.gov/pubmed/6492758.

Pirotzky, E., Bidault, J., Burtin, C., Gubler, M.C., Benveniste, J., 1984b. Release of platelet-activating factor, slow-reacting substance, and vasoactive amines from isolated rat kidneys. Kidney Int. 25, 404–410. https://doi.org/10.1038/ki.1984.31.

Pirotzky, E., Page, C., Morley, J., Bidault, J., Benveniste, J., 1985. Vascular permeability induced by Paf-acether (platelet-activating factor) in the isolated perfused rat kidney. Agents Actions 16, 17–18. https://doi.org/10.1007/BF01999630.

Ratcliffe, P.J., Pukrittayakamee, S., Ledingham, J.G.G., Warrell, D.A., 1989. Direct nephrotoxicity of Russell's viper venom demonstrated in the isolated perfused rat kidney. Am. J. Trop. Med. Hyg. 40, 312–319. https://doi.org/10.4269/ajtmh.1989.40.312.

Rossier, B.C., Stutts, M.J., 2009. Activation of the epithelial sodium channels (ENaC) by serine proteases. Annu. Rev. Physiol. 71, 361–379. https://doi.org/10.1146/annurev.physiol.010908.163108.

Schlondorff, D., Neuwirth, R., 1986. Platelet-activating factor and the kidney. Am. J. Physiol. Ren. Physiol. 251, F1–F11. https://doi.org/10.1152/ajprenal.1986.251.1.F1.

Schlondorff, D., Goldwasser, P., Neuwirth, R., Satriano, J.A., Clay, K.L., 1986. Production of platelet-activating factor in glomeruli and cultured mesangial cells. Am. J. Physiol. 250, F1123–F1127. https://doi.org/10.1152/ajprenal.1986.250.6.F1123.

Schwertschlag, U., Scherf, H., Gerber, J.G., Mathias, M., Nies, A.S., 1987. L-platelet activating factor induces changes on renal vascular resistance, vascular reactivity, and renin release in the isolated perfused rat kidney. Circ. Res. 60, 534–539. https://doi.org/10.1161/01.res.60.4.534.

Sharma, M., Das, D., Iyer, J.K., Kini, R.M., Doley, R., 2015. Unveiling the complexities of *Daboia russelii* venom, a medically important snake of India, by tandem mass spectrometry. Toxicon 107, 266–281. https://doi.org/10.1016/j.toxicon.2015.06.027.

Sitprija, V., Benyajati, C., Boonpucknavig, V., 1974. Further observations of renal insufficiency in snake bite. Nephron 13, 396–403. https://doi.org/10.1159/000180416.

Sitprija, V., Chaiyabutr, N., 1999. Nephrotoxicity in snake envenomation. J. Nat. Toxins 8, 271–277. PMID: 10410337.

Sitprija, V., Sitprija, S., 2012. Renal effects and injury induced by animal toxins. Toxicon 60, 943–953. https://doi.org/10.1016/j.toxicon.2012.06.012.

Smith, H.W., 1962. Principle of Renal Physiology. Oxford University Press, New York, pp. 196–217.

Smith, K.A., Cornett, L.E., Norris, J.S., Byers, L.W., Muirhead, E.E., 1982. Blockade of alpha-adrenergic receptors by analogues of phosphatidylcholine. Life Sci. 31, 1891–1902. https://doi.org/10.1016/0024-3205(82)90027-3.

Snyder, F., Fitzgerald, V., Blank, M.L., 1996. Biosynthesis of platelet-activating factor and enzyme inhibitors. Adv. Exp. Med. Biol. 416, 5–10. https://doi.org/10.1007/978-1-4899-0179-8_2.

Snyder, F., 1985. Chemical and biochemical aspects of platelet activating factor: a novel class of acetylated ether-linked choline-phospholipids. Med. Res. Rev. 5, 107–140. https://doi.org/10.1002/med.2610050105.

Suwansrinon, K., Khow, O., Mitmoonpitak, C., Daviratanasilpa, S., Chaiyabutr, N., Sitprija, V., 2007. Effects of Russell's viper venom fractions on systemic and renal hemodynamics. Toxicon 49, 82–88. https://doi.org/10.1016/j.toxicon.2006.09.013.

Swe, T.N., Kyaw, K.M., Win, H., Win, K., Htwe, T.T., 1997. Russel's viper venom fractions and nephrotoxicity. Southeast Asian J. Trop. Med. Publ. Health 28, 657–663. PMID: 9561625.

Taft, D.R., 2004. The isolated perfused rat kidney model: a useful tool for drug discovery and development. Curr. Drug Discov. Technol. 1, 97–111. https://doi.org/10.2174/1570163043484824.

Tan, K.Y., Tan, N.H., Tan, C.H., 2018. Venom proteomics and antivenom neutralization for the Chinese eastern Russell's viper, *Daboia siamensis* from Guangxi and Taiwan. Sci. Rep. 8, 8545. https://doi.org/10.1038/s41598-018-25955-y.

Tan, N.H., Fung, S.Y., 2009. Snake venom L-amino acid oxidase. In: Mackessy, S.P. (Ed.), Handbook of Venoms and Toxins of Reptiles, first ed. CRC Press, pp. 219–232.

Tasoulis, T., Isbister, G.K., 2017. A review and database of snake venom proteomes. Toxins 9, 290. https://doi.org/10.3390/toxins9090290.

Thamaree, S., Sitprija, V., Tongvongchai, S., Chaiyabutr, N., 1994. Changes in renal hemodynamics induced by Russell's viper venom: effects of Indomethacin. Nephron 67, 209–213. https://doi.org/10.1159/000187930.

Tolins, J.P., Vercellotti, G.M., Wilkowske, M., Ha, B., Jacob, H.S., Raij, L., 1989. Role ofplatelet activating factor in endotoxemic acute renal failure in the male rat. J. Lab. Clin. Med. 113, 316–324. https://www.translationalres.com/article/0022-2143(89)90094-2/pdf.

Tungthanathanich, P., Chaiyabutr, N., Sitprija, V., 1986. Effect of Russell's viper (*Vipera russelli siamensis*) venom on renal hemodynamics in dogs. Toxicon 24, 365–371. https://doi.org/10.1016/0041-0101(86)90196-0.

Wang, J., Dunn, M.J., 1987. Platelet-activating factor mediates endotoxin-induced acute renal insufficiency in rats. Am. J. Physiol. Ren. Physiol. 253, F1283–F1289. https://doi.org/10.1152/ajprenal.1987.253.6.F1283.

Weisman, S.M., Felsen, D., Vaughan Jr., E.D., 1985. Platelet-activating factor is a potent stimulus for renal prostaglandin synthesis: possible significance in unilateral ureteral obstruction. J. Pharmacol. Exp. Therapeut. 235 (1), 10–15. PMID: 3862805.

Weisman, S.M., Freund, R.M., Felsen, D., Vaughan Jr., E.D., 1988. Differential effect of platelet-activating factor (PAF) receptor antagonists on peptide and PAF- stimulated prostaglandin release in unilateral ureteral obstruction. Biochem. Pharmacol. 37 (15), 2927–2932. https://doi.org/10.1016/0006-2952(88)90277-8.

Whatley, R.E., Nelson, P., Zimmerman, G.A., Stevens, D.L., Parker, C.J., McIntyre, T.M., Prescott, S.M., 1989. The regulation of platelet-activating factor production in endothelial cells. J. Biol. Chem. 264, 6325–6333. PMID: 2703492.

Willinger, C.C., Thamaree, S., Schramek, H., Gstraunthaler, G., Pfaller, W., 1995. In vitro nephrotoxicity of Russell's viper venom. Kidney Int. 47, 518–528. https://doi.org/10.1038/ki.1995.65.

Win-Aung, Sein-Sein-May, Aung-Myat-Kyaw, Baby-Hla, Aye-Kyaw, 1998. Effects of Russell's viper venom on renal lysosomal functions in experimental mice. Toxicon 36, 495–502. https://doi.org/10.1016/S0041-0101(97)00110-4.

Worthington Enzyme Manual, 1977. L-amino Acid Oxidase. Worthington Biochemical Corp., USA, pp. 49–50.

Young, M.K., Raisz, L.G., 1952. An anthrone procedure for determination of inulin in biological fluids. Proc. Soc. Exp. Biol. Med. 80, 771–774. https://doi.org/10.3181/00379727-80-19758.

Yoshida, M., Ueda, S., Soejima, H., Tsuruta, K., Ikegami, K., 1986. Effects of prostaglandin E2 and I2 on renal cortical and medullary blood flow in rabbits. Arch. Int. Pharmacodyn. Ther. 282 (1), 108–117. PMID: 3532982.

Zuliani, J.P., Kayano, A.M., Zaqueo, K.D., Neto, A.C., Sampaio, S.V., Soares, A.M., Stábeli, R.G., 2009. Snake venom L-amino acid oxidases: some consideration about their functional characterization. Protein Pept. Lett. 16, 908–912. https://doi.org/10.2174/092986609788923347.